



Cite this: *RSC Adv.*, 2023, 13, 990

Received 24th October 2022  
Accepted 5th December 2022

DOI: 10.1039/d2ra06726a

rsc.li/rsc-advances

## Vinyl azides in organic synthesis: an overview

Fateme Gholami,<sup>a</sup> Faeze Yousefnejad,<sup>a</sup> Bagher Larijani<sup>b</sup>  
and Mohammad Mahdavi<sup>id</sup>\*<sup>b</sup>

Among organic azides, vinyl azides have attracted significant attention, because of their unique properties in organic synthesis, which led to reports of many types of research on this versatile conjugated azide in recent years. This magical precursor can also be converted into intermediates such as iminyl radicals, 2*H*-azirines, iminyl metal complexes, nitrilium ions, and iminyl ions, making this compound useful in heterocycle synthesis.

### Introduction

Vinyl azides are versatile building blocks in which a double bond is attached directly to the azide group.<sup>1</sup> One reason for the great importance of vinyl azides in organic chemistry is the application of this compound to the synthesis of a large number of nitrogen-containing heterocycles, such as pyrazoles, pyrroles, imidazoles, thiazoles, triazoles, pyridines, quinolines, isoquinolines, and imidazo[1,2-*a*]pyridines (Fig. 1).<sup>2,3</sup>

There are different types of cyclization pathway for vinyl azides, like the azirine pathway, carbodiimide pathway, and initial alkenyl group, which can be seen in Scheme 1.<sup>4</sup>

The versatility of vinyl azides in organic synthesis has long been known. Photolysis, thermolysis, cycloaddition, and reaction with nucleophiles and electrophiles are common processes that vinyl azides can go through. The double bond in this compound also causes the azide to be more reactive with other functional groups. It is found that the addition of an external radical species causes the production of an iminyl radical that undergoes numerous transformations (Fig. 2).  $\alpha$ -Substituted vinyl azides have been utilized as radical acceptors to produce a variety of molecules, including  $\alpha$ -trifluoro methylated ketones,  $\alpha$ -trifluoromethyl azines, keto sulfones,  $\alpha$ -azido styrene, cyclic  $\beta$ -amino ketones, *N*-unprotected enamines, enaminones,  $\beta$ -keto phosphine oxides, unsymmetrical ketones, and 2-aryacetophenones.<sup>5</sup>

It has also been observed that vinyl azides can serve as multipurpose precursors for the synthesis of various units through diverse cleavages. Units generated from different cleavages are shown in Fig. 3.<sup>2</sup>

Vinyl azide decomposition has been the subject of several investigations. Thermal decomposition of vinyl azides gives different products (depending on substituents): in most cases,

internal vinyl azides give azirine intermediates.<sup>6</sup> It is found that thermolysis and photolysis of internal vinyl azides produce azirines in good yields, and sometimes with a small amount of iminoketenes (Scheme 2). In rare cases, ketene imines are major products of this type of reaction.<sup>1</sup>

In Scheme 3 two mechanistic pathways for the transformation of vinyl azide to azirine (**A**  $\rightarrow$  **B**) are shown. The vinyl azides can either release nitrogen to generate vinyl nitrene and then cyclize to the azirine (path a), or can decompose with simultaneous ring closure to generate **B** directly (pathway b).<sup>7</sup>

Smolinsky, who first pyrolyzed vinyl azides to azirines, considered the possibility that vinyl azides would decompose to azirine *via* an unstable isotriazole intermediate (path C) (Scheme 4).<sup>7</sup>

A computational study on vinyl azide decomposition was also done by da Silva *et al.* in 2014. Electronic structural calculations showed that the decomposition of the *s-cis* conformer of vinyl azide leads to the generation of ketenimine *via* a single-step conversion: *s-cis*-CH<sub>2</sub>CHN<sub>3</sub>  $\rightarrow$  CH<sub>2</sub>CNH + N<sub>2</sub> while the transformation of the *s-trans* conformer to acetonitrile happens in two steps: *s-trans*-CH<sub>2</sub>CHN<sub>3</sub>  $\rightarrow$  cyc-CH<sub>2</sub>NCH + N<sub>2</sub>  $\rightarrow$  CH<sub>3</sub>CN + N<sub>2</sub>.<sup>6</sup>

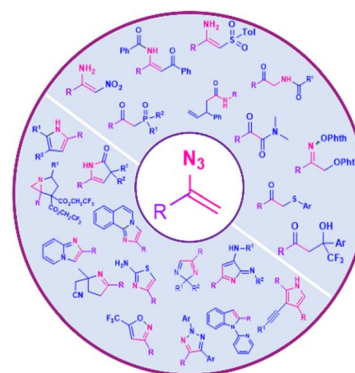
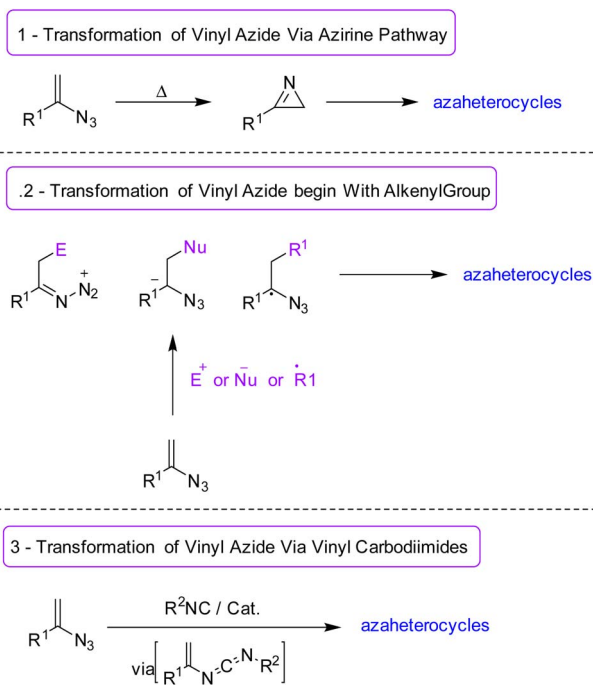


Fig. 1 Examples of compounds produced by vinyl azides.

<sup>a</sup>School of Chemistry, College of Science, University of Tehran, Tehran, Iran

<sup>b</sup>Endocrinology and Metabolism Research Center, Endocrinology and Metabolism Clinical Sciences Institute, Tehran University of Medical Sciences, Tehran, Iran.  
E-mail: momahdavi@tums.ac.ir





Scheme 1 Cyclization pathways of vinyl azides.

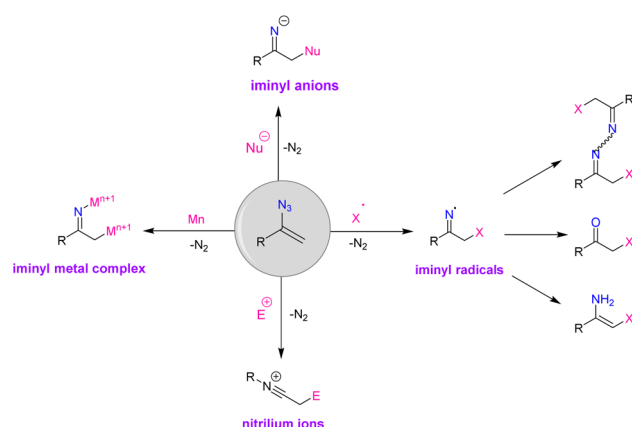


Fig. 2 Conversion of vinyl azide to different intermediates.

Results of their calculations indicate that the *s-cis* ( $\theta_{CCNN} = 0.0^\circ$ ) and *s-trans* ( $\theta_{CCNN} = 180.0^\circ$ ) conformers of vinyl azide have analogous relative energetic stabilities. Furthermore, in an experimental microwave study, the *s-cis* conformer was declared to be a bit more stable than the *s-trans* by  $0.460 \text{ kcal mol}^{-1}$ .<sup>8</sup> Because of the very small energy difference between these conformers, fast interconversion is anticipated.<sup>6</sup>

According to the calculations, the decomposition of vinyl azides in the singlet state can go through two different reaction pathways, as shown in Scheme 5, beginning from *s-cis* or *s-trans*-vinyl azide. Ketenimine ( $CH_2CNH$ ) is generated through single-step conversion of the *s-cis* conformer. The transition state for the *s-cis*- $CH_2CHN_3 \rightarrow CH_2CNH$  reaction (**2T**) is  $37.78 \text{ kcal mol}^{-1}$  ( $47.92 \text{ kcal mol}^{-1}$  at MP2/6-311++G(d,p) level) higher in energy than *s-cis*- $CH_2CHN_3$  (**1**). Meanwhile, conversion of the *s-trans*

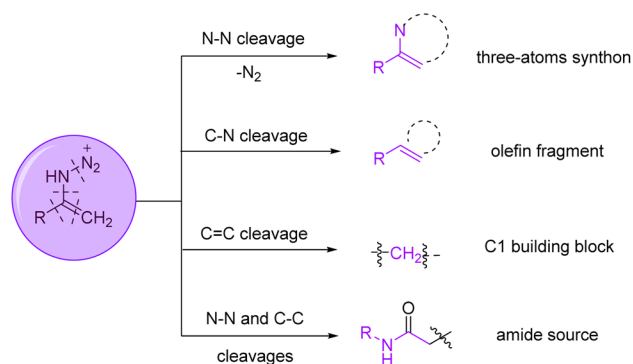
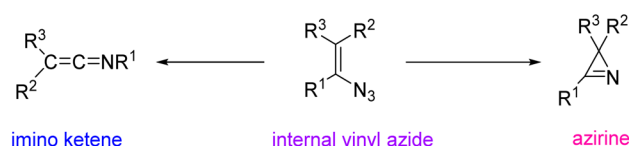
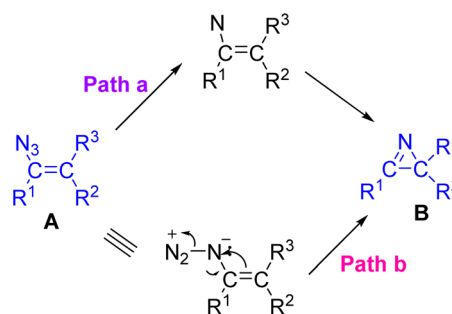


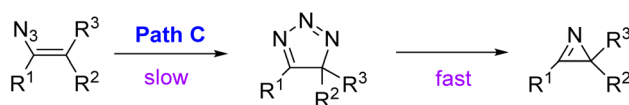
Fig. 3 Vinyl azide as a multipurpose precursor.



Scheme 2 Formation of azirine and iminoketene from internal vinyl azide.



Scheme 3 Two mechanistic pathways for the transformation of vinyl azide to azirine.

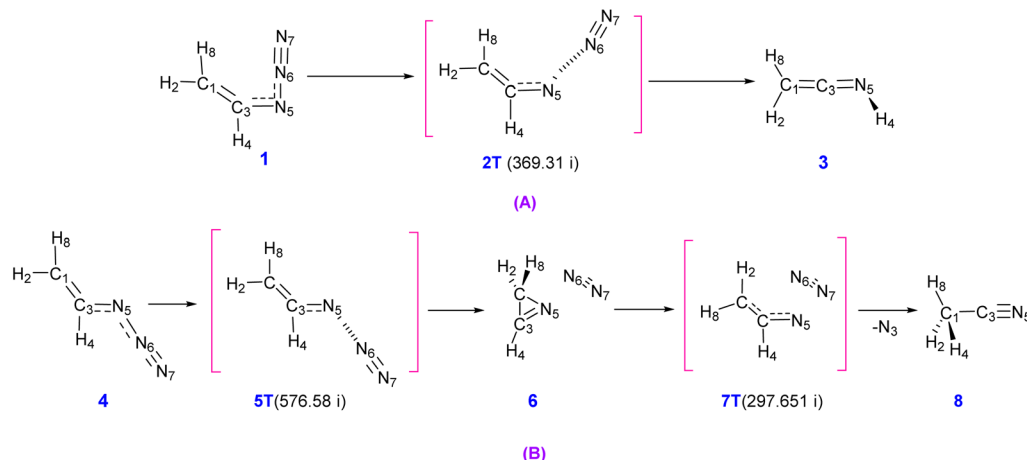


Scheme 4 Pyrolyze of vinyl azide.

conformer to acetonitrile happens in two steps: *s-trans*- $CH_2CHN_3 \rightarrow \text{cyc-}CH_2NCH + N_2 \rightarrow CH_3CN + N_2$ . The transition state between *s-trans*- $CH_2CHN_3$  and *cyc-}CH\_2NCH*-(2*H*-azirine) (**5T**) is  $33.90 \text{ kcal mol}^{-1}$  ( $41.89 \text{ kcal mol}^{-1}$  at MP2/6-311++G(d,p) level) higher than *s-trans*- $CH_2CHN_3$ , while the transition state between acetonitrile and 2*H*-azirine (**7T**) is  $49.93 \text{ kcal mol}^{-1}$  ( $68.55 \text{ kcal mol}^{-1}$  at MP2/6-311++G(d,p) level) higher than 3*H*-azirine (Fig. 4).<sup>6</sup>

From the analysis of da Silva and coworker it can be deduced that  $N_2$ , 2*H*-azirine, acetonitrile and ketenimine are generated from the decomposition of vinyl azide in the singlet state. It is





**Scheme 5** Multistep reaction for the decomposition of vinyl azide in the singlet state: (A) decomposition of *s-cis*, (B) decomposition of *s-trans*. For the transition states we show in parentheses the values of imaginary frequencies (in  $\text{cm}^{-1}$ ).

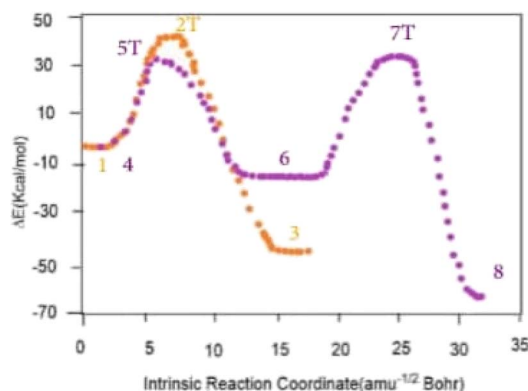
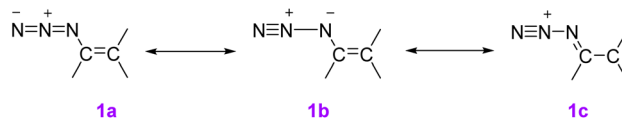


**Fig. 4** Full energy profile of the IRC path calculated for the decomposition of *s-cis*-vinyl azide (orange points) and *s-trans*-vinyl azide (purple points) at B3LYP/6-311++G(d,p) level.



**Fig. 5** Singlet and triplet vinyl nitrene.

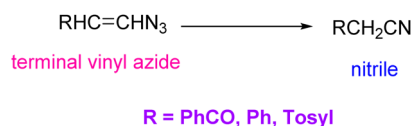


**Scheme 7** Resonance forms of vinyl azide.

also known that the decomposition mechanism of organic azide includes a nitrene species corresponding to a TS localized at a point of intersystem crossing (ISC) between singlet ( $^1\text{S}$ ) and triplet ( $^3\text{S}$ ) surfaces.<sup>6</sup>

Vinyl azides can also be good precursors for the synthesis of nitrile compounds.<sup>9</sup> In the synthesis of nitrile from terminal vinyl azide, the decomposition of vinyl azide first produces iminoketene; then, the latter product is tautomerized to the more stable nitrile (Scheme 6).<sup>1</sup>

Vinyl nitrene is also proposed as an intermediate for the chemistry of vinyl azides. The former compound can be singlet or triplet (Fig. 5). They can also act as a three-atom C–C–N synthon in cycloaddition reactions.<sup>10</sup>



**Scheme 6** Formation of nitrile from terminal vinyl azide.

In an investigation of the stability of vinyl azides, it is important to pay attention to the point that the azide group in vinyl azide increases the electron density at the  $\beta$  carbon atom. This means, that canonical structure 1C makes an extreme contribution to the overall stabilization of azide with the result that the order of the  $\text{N}_2$ –N bond that cleaves on thermolysis is less than 1.5 (Scheme 7). Gerrit Labbe and coworkers showed that vinyl azides exhibit moderate energies of activation and low entropies of activation, consistent with the nitrene pathway.<sup>7,11</sup>

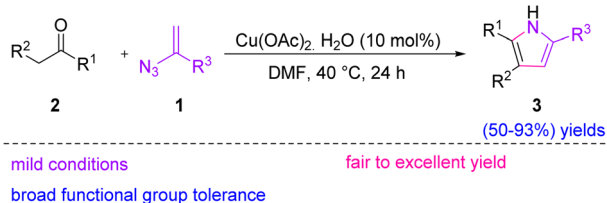
Todeschini and coworker, in 1978, compared the net charge of  $\text{N}_1$  in *cis* and *trans* forms of vinyl azides. The net charge understood on  $\text{N}_1$  ( $-0.388$  in the *trans* form and  $-0.396$  in the *cis* form) and on  $\text{N}_3$  ( $-0.299$  in *trans* and  $-0.294$  in *cis*) confirm the suggestion that the resonance form of covalently bonded azides ( $\text{R-N}=\text{N}^+=\text{N}^-$ ) is more stable in the *trans* conformation, while ( $\text{R-N}=\text{N}^+\equiv\text{N}$ ) is more stable in the *cis* conformation.<sup>12</sup>

## Formation of 5-membered heterocycles

In 2015, Donthiri *et al.* proposed a novel strategy for the synthesis of substituted 1*H*-pyrroles 3 through the copper-



## Review

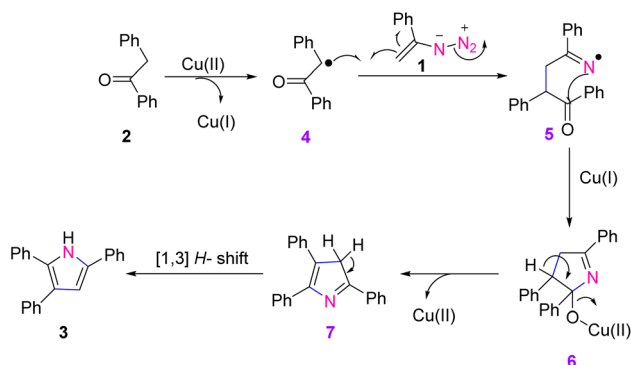


**Scheme 8** Synthesis of substituted 1H-pyrroles **3** through copper-catalyzed  $\text{C}(\text{sp}^3)\text{--H}$  functionalization of ketones **2**.

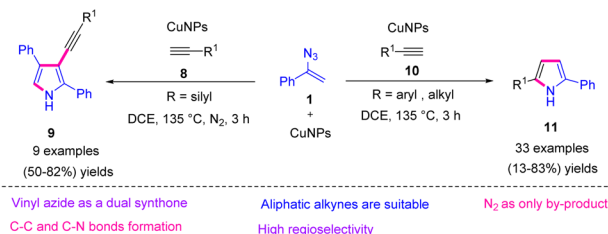
catalyzed  $\text{C}(\text{sp}^3)\text{--H}$  functionalization of ketones **2** with vinyl azides **1**. Their method efficiently accessed a series of 2,3,5-trisubstituted-1H-pyrroles in fair to excellent yields (50–93%).<sup>13</sup> Pyrroles are considered as specific heterocycles due to their application in biological systems and their remedial activities. Pharmaceuticals such as potent blockers for potassium-competitive acid, anti-tumor agents, the leading cholesterol-lowering drug Lipitor, and a wide range of natural products are constituted with a pyrrole core structure.<sup>14,15</sup> Pyrroles also serve as useful building blocks in the synthesis of bioactive compounds (Scheme 8).<sup>16</sup>

To explain the mechanism of this reaction, deoxy benzoin **2** in the presence of  $\text{Cu}(\text{II})$  first generated a radical intermediate **4**, and  $\text{Cu}(\text{II})$  transformed into  $\text{Cu}(\text{I})$ . Intermediate **4** in the presence of vinyl azides **1**, gave iminyl radical intermediate **5**. Next, the latter compound instantly underwent a radical addition and gave  $\text{Cu}(\text{II})$  complex intermediate **6**. In the final step, abstraction of  $\text{Cu}(\text{II})$  followed by [1,3]-H shift, gave the final product **3** (Scheme 9).<sup>13</sup>

In 2019, Jiang *et al.* synthesized substituted pyrroles **9** and **11** by utilizing vinyl azides **1** and terminal alkynes **8** and **10** in the presence of a nano copper catalyst. By using this strategy, the research group synthesized 2,5-disubstituted pyrroles **11** in poor to very good yields (13–83%) and 2,3,4-trisubstituted pyrroles **9** in fair to very good yields (50–82%).<sup>17</sup> In this project, Jiang and coworkers observed switchable reactions by varying the substituent *R* of the terminal alkyne. This transition-metal-catalyzed C–C and C–N bond formation is a necessary tool in organic synthesis, allowing for the construction of basis



**Scheme 9** Mechanism for the synthesis of substituted 1H-pyrroles **3** through copper-catalyzed  $\text{C}(\text{sp}^3)\text{--H}$  functionalization of ketones **2**.



**Scheme 10** Synthesis of substituted pyrroles **9** and **11** through switchable reactivity between vinyl azides **1** and terminal alkynes **8** and **10**.

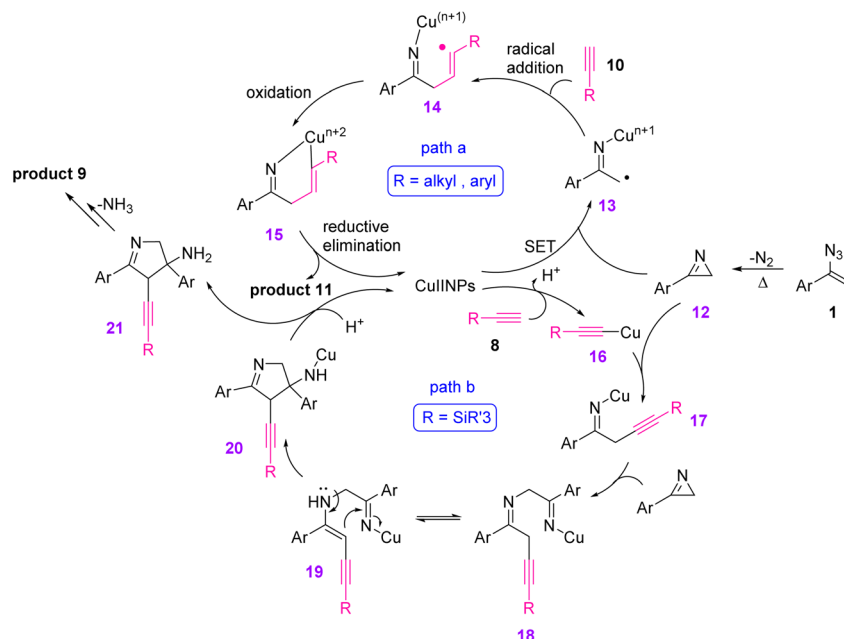
backbones which are popular building blocks of active molecules in the material sciences (Scheme 10).<sup>18,19</sup>

To illustrate the mechanism, the vinyl azides **1** underwent thermal decomposition to generate 2H-azirine **12**. In pathway **A** for the generation of the 2,5-disubstituted pyrrole **11**, 2H-azirine first underwent an SET reduction with  $\text{CuNPs}$  to give iminyl  $\text{Cu}(\text{II})$  intermediate **13**. This C-radical was trapped by terminal alkyne **10** through intermolecular addition to give intermediate **14**. Then, the radical was captured by intramolecular copper(II) to generate copper adduct **15**, which underwent reductive elimination to reproduce the active copper and gave the 3H-pyrroles. Eventually, 2,5-disubstituted pyrrole **11** was produced through the isomerization of the 3H-pyrrole (Scheme 11).

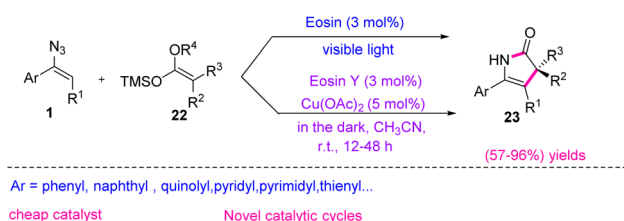
In path **B** for the synthesis of 2,3,4-trisubstituted pyrrole **9**,  $\text{CuNPs}$  first reacted with the terminal alkyne **8** to generate copper acetylide **16**. Then, 2H-azirine underwent a nucleophilic ring opening with copper acetylide **16**, giving iminyl copper intermediate **17**, which was protonated to generate the NH imine. In the next step, the iminyl copper intermediate **17** reacted with another 2H-azirine, generating intermediates **18** and **19**, which are keto–enol tautomers. The intramolecular cyclization of **18** generated intermediate **20**, which underwent protonolysis to release intermediate **21** along with copper. Further elimination of  $\text{NH}_3$  and isomerization produced the desired product **9** (Scheme 11).<sup>17</sup>

In 2018, Liu *et al.* utilized a copper-catalyzed dark reaction with eosin Y to produce ene- $\gamma$  lactams **23** (Scheme 12). Eosin Y is a common organo-photocatalyst in visible-light photo-redox processes. It showed excellent catalytic activities for thermal redox reactions in the presence of a catalytic amount of  $\text{Cu}(\text{OAc})_2$ . With this catalytic system, ketene silyl acetals **22** and vinyl azides **1** combined through [3 + 2]-cycloadducts, resulting in the production of ene- $\gamma$ -lactams **23** in fair to excellent yields (57–96%).<sup>20</sup> Ene- $\gamma$ -lactams are important synthons as they are broadly used in the synthesis and key structural elements of many bioactive natural products and medicinally relevant compounds.<sup>21</sup> The electron-rich enamine scaffolds of ene- $\gamma$ -lactams, as highly versatile intermediates, could take part in a hetero-Diels–Alder<sup>22</sup> reaction or [3 + 2]-cyclization with  $\alpha,\beta$ -unsaturated carbonyl compounds, producing tetrahydropyranopyrazole or enantioenriched bicyclic  $\gamma$ -lactams. Ene- $\gamma$ -lactams could also react with electrophilic aldehydes to produce fused bicycles.<sup>23</sup>



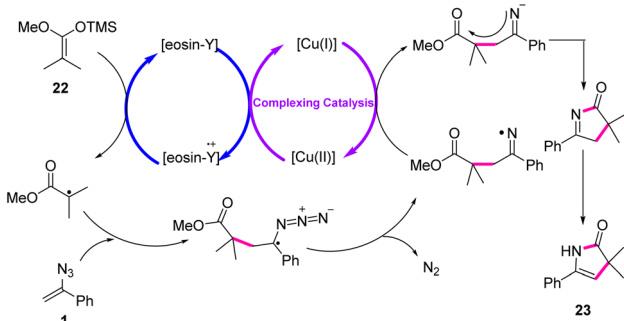


Scheme 11 Mechanism for the Cu-catalyzed synthesis of pyrroles **9** and **11** from vinyl azides **1** and alkyne.

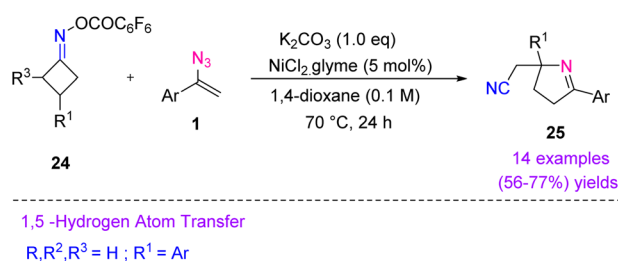


Scheme 12 Synthesis of ene- $\gamma$  lactams **23** from vinyl azides **1**.

To explain the mechanism, the initial reaction between  $\text{Cu}(\text{OAc})_2$  and eosin Y would give an eosin Y radical cation, which would be capable of oxidizing the ketene silyl acetal through single electron transfer (SET) to  $\alpha$ -ester radicals. Addition of  $\alpha$ -ester radicals to vinyl azides **1** would give the iminyl radical and dinitrogen. The resulting iminyl radicals should afterward be reduced by low-valent  $\text{Cu}(\text{I})$ , thus generating iminyl anions and regenerating  $\text{Cu}(\text{II})$ . Eventually, the



Scheme 13 Mechanism for the synthesis of ene- $\gamma$  lactams **23** from vinyl azides **1**.



Scheme 14 Synthesis of cyano-alkylated 3,4-dihydro-2H-pyrroles **25** through reaction of vinyl azides **1** and cycloketone oxime esters **24**.

intramolecular nucleophilic substitution of iminyl anion to ester after isomerization produced final products **23** (Scheme 13).<sup>20</sup>

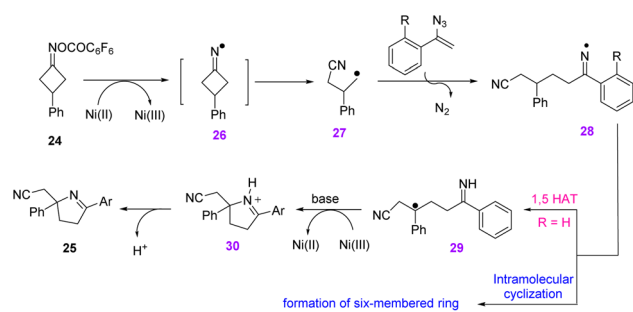
In 2019, Guo *et al.* reported Ni-catalyzed ring-opening/radical addition/ring-closing of cycloketone oxime esters and vinyl azides (Scheme 14). Their protocol resulted in fast access to cyano-alkylated 3,4-dihydro-2H-pyrroles **25** (five-membered ring) in fair to good yields (56–77%).<sup>24</sup>

To describe the mechanism, Ni-mediated single-electron reduction of cyclobutanone oxime ester **24** first generated iminyl radical **26**, which underwent C–C bond cleavage and led to the formation of cyano-alkyl radical **27**. The latter radical reacted with the C=C bond of vinyl azide, producing iminyl radical **28** by releasing  $\text{N}_2$ . For aryl vinyl azides, iminyl radical **28** proceeded through 1,5-H-transfer to generate radical **29**. Oxidation, cyclization, and then deprotonation of **29** gave desired product **25** (Scheme 15).<sup>24</sup>

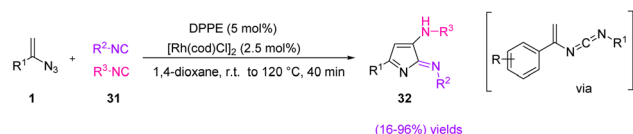
In 2019, Zhang *et al.* achieved novel 2H-pyrrol-2-imine derivatives **32** in a one-pot process through a rhodium-catalyzed reaction of vinyl azides **1** and two equivalent







**Scheme 15** Mechanism for the synthesis of cyano-alkylated 3,4-dihydro-2H-pyrroles **25** from vinyl azide **1**.

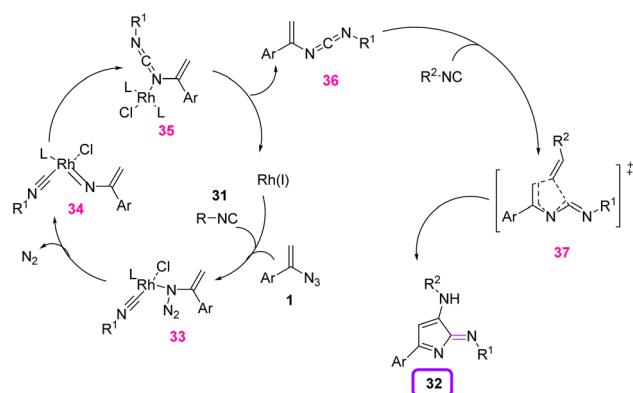


**Scheme 16** Synthesis of 2H-pyrrole-2-imine derivatives **32** from isocyanide **31** and vinyl azides **1**.

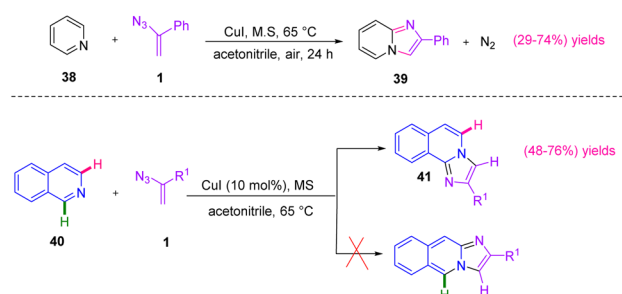
amounts of isocyanide **31** (Scheme 16). Their method offered facile access to 3-amino-5-aryl-2H-pyrrol-2-imines bearing different substitutions on the nitrogen in poor to excellent yields (16–96%).<sup>25</sup> 2H-Pyrrole is a significant structural motif present in a broad range of natural products and biologically active compounds.<sup>26,27</sup>

A plausible mechanism consists of two processes: Rh(I)-catalyzed cross-coupling of vinyl azides **1** with the first isocyanide **31**, and the cyclization of the vinyl carbodiimide with the second isocyanide. Vinyl carbodiimide **36** was first generated through an Rh-nitrene pathway with the release of N<sub>2</sub>. In the next step, thermal cyclization of the second isocyanide generated 2H-pyrrol-2-imine **32** as the product (Scheme 17).<sup>25</sup>

In 2014, Bairagi *et al.* came up with a new approach to synthesize imidazole heterocycles (Scheme 18). In this study, by utilizing copper-catalyzed C–H functionalization of pyridine and isoquinoline, the research group synthesized derivatives of



**Scheme 17** Mechanism for the Rh(I)-catalyzed synthesis of 2H-pyrrol-2-imine derivatives **32**.

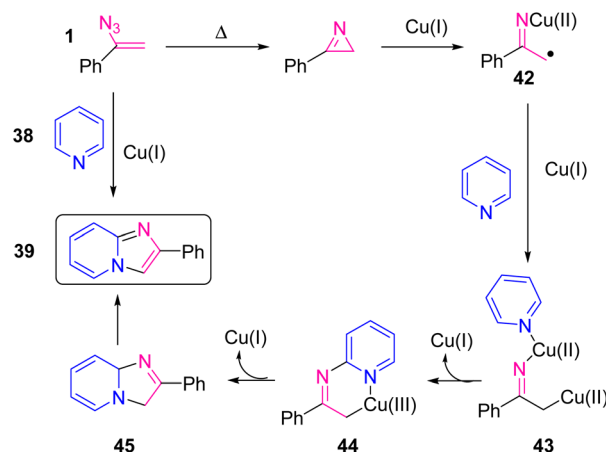


**Scheme 18** Cu-catalyzed synthesis of imidazo[1,2-a]pyridines **39** and imidazole[2,1-a]isoquinoline **41** derivatives.

**39** in poor to good yields (29–74%) and **41** in poor to good yields (48–76%).<sup>28</sup> The development of an efficient strategy for the synthesis of azaheterocycles *via* direct functionalization of C–H bonds utilizing transition metal catalysts is a highly important subject in organic chemistry. Imidazo[1,2-a]pyridines **39** are aza heterocycles that have received a lot of attention due to their diverse biological activities.<sup>29,30</sup>

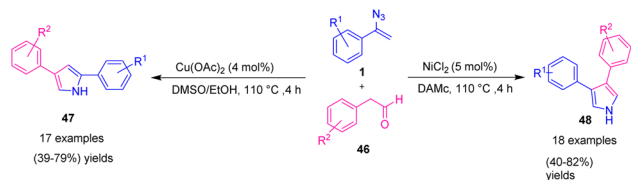
Scheme 19 provides plausible information about the mechanism of the reaction. Vinyl azides **1** first underwent thermal decomposition to generate the 2H-azirine, which gave iminylcopper(II) radical intermediate **42** in the presence of Cu(I), with homolytic cleavage of the C–N bond. Then intermediate **42** generated intermediate **43**. Oxidative cyclization of **43** gave Cu(III) complex **44**, and reductive elimination followed by oxidation produced the final product.<sup>28</sup>

In 2012, Jiao *et al.* developed an innovative and effective method to synthesize 2,4-disubstituted pyrrole **47** and 3,4-disubstituted pyrrole **48** by copper and nickel catalysts (Scheme 20).<sup>31</sup> Pyrroles are a significant class of heterocyclic compound; they are also building blocks in many natural products,<sup>32</sup> synthetic pharmaceutical compounds,<sup>15</sup> and material science.<sup>33</sup> Compared with previous acidic or basic conditions for poly-substituted pyrrole synthesis, the conditions were mild, neutral, and did not involve any additive. They resulted in



**Scheme 19** Mechanism for the Cu-catalyzed synthesis of imidazo[1,2-a]pyridines **39**.



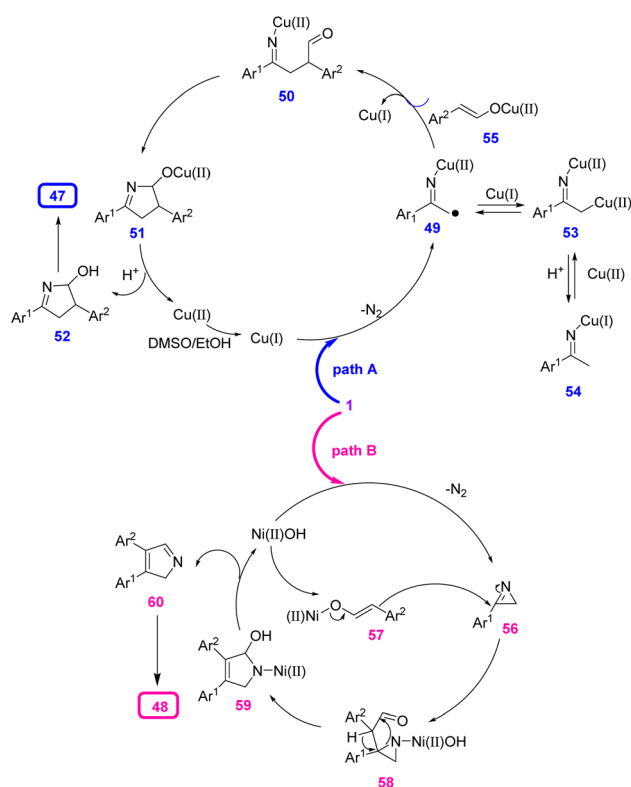


**Scheme 20** Copper and nickel catalyzed reaction between vinyl azides **1** and phenyl acetaldehyde **46**.

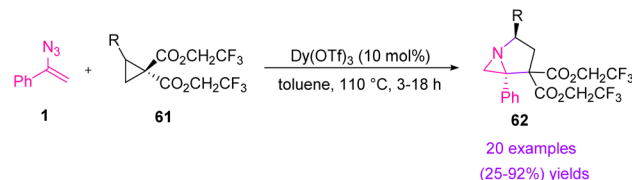
the synthesis of 2,4-disubstituted pyrrole in poor to good yields (39–79%) and 3,4-disubstituted pyrrole in poor to very good yields (40–82%).<sup>31</sup>

For the Cu-catalyzed formation of 2,4-disubstituted pyrrole **47** (path **A**), Cu(OAc)<sub>2</sub> might first be reduced by DMSO/EtOH to generate Cu(I) or through disproportionation to generate Cu(I). In the next step, radical intermediates **49** were produced through a denitrogenative decomposition of the vinyl azides **1**. Then, the radical coupling of intermediate **49** with enol tautomers of the phenylacetaldehydes produced intermediates **50**, which underwent nucleophilic attack on the aldehyde, leading to the addition of intermediates **51**. Subsequent protonation gave intermediates **52**, and dehydration of intermediates **52** produced 2,4-disubstituted pyrroles **47** (Scheme 21).

For the Ni-catalyzed production of 3,4-disubstituted pyrrole **48** (path **B**), NiCl<sub>2</sub> first promoted the decomposition of vinyl azides **1** to give 2*H*-azirines **56**, which could not be generated in



**Scheme 21** Proposed mechanism for the synthesis of 2,4- and 3,4-disubstituted pyrroles **47** and **48** from vinyl azides **1**.

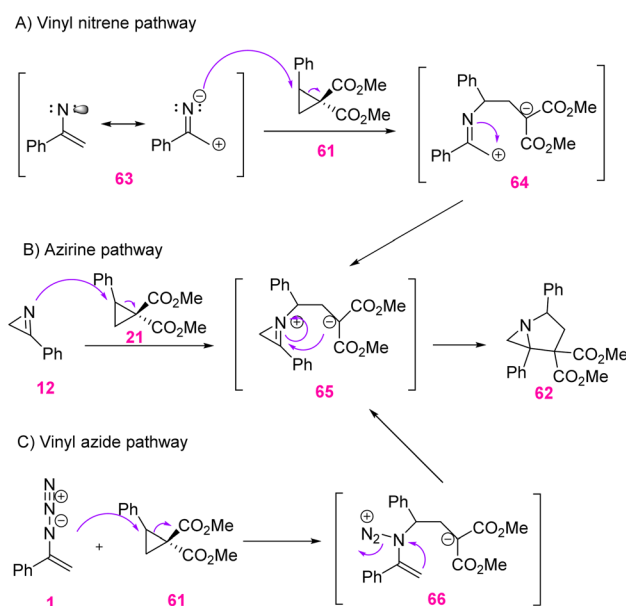


**Scheme 22** Annulation reaction of donor–donor–acceptor cyclopropanes **61** with vinyl azides **1**.

the presence of a Cu catalyst. In the next step, nucleophilic attack by the enol tautomers of phenylacetaldehydes generated intermediates **58**. Ring-opening of intermediates **58** gave five-membered species **59**. β-OH elimination gave the 2*H*-pyrroles **60** and Ni complexes, which reacted with the aldehyde to regenerate enol intermediate **57**. In the final step, 3,4-disubstituted pyrroles **48** were produced through tautomerization of intermediates **60** (Scheme 21).<sup>31</sup>

The field of donor–acceptor cyclopropane chemistry has seen significant resurgence since the early work of Wenkert, Danishefsky, and Reissig. In 2016, Kerr *et al.* utilized donor–acceptor cyclopropanes and (1-azidovinyl) benzene **1** to synthesize **62** (Scheme 22). Under the influence of Lewis acid and heat, donor/acceptor cyclopropanes underwent an annulation reaction with (1-azidovinyl)benzene and produced an unusual azabicyclic scaffold of **62** in poor to excellent yield (25–92%).<sup>34</sup>

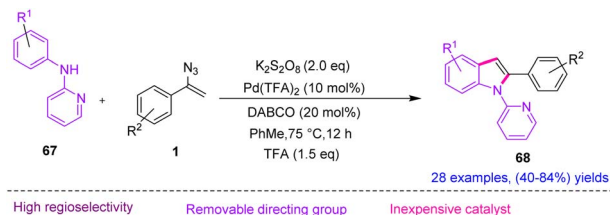
Three possible mechanistic explanations for the observed transformation are shown in Scheme 23. Option **A** involves vinyl nitrene formation by the thermolysis of vinyl azides **1**. Nitrene **63** may be assumed to behave as a dipolar species in the Lewis-acid-mediated ring opening of cyclopropane **61** to generate **64**. Conversion of **64** to the more stable iminium ion **65** established



**Scheme 23** Mechanism for the annulation reaction of donor–donor–acceptor cyclopropanes **61** with vinyl azides **1**.



## Review



Scheme 24 Synthesis of 2-arylindole **68** through the Pd-catalyzed reaction of vinyl azides **1**.

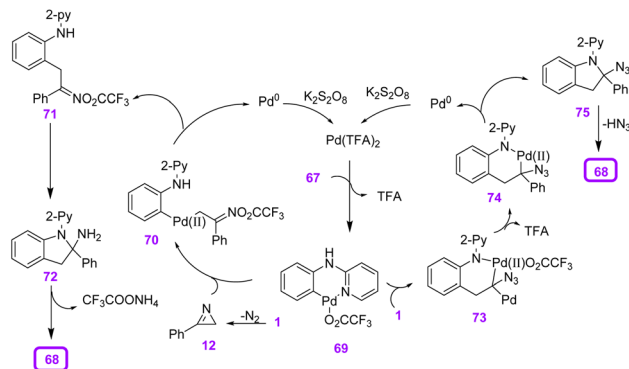
a Mannich-style ring closure to produce **62**. Option **B** involved an azirine formation by the thermolysis of the vinyl azide through a putative nitrene **63**. Ring opening of the cyclopropane by nucleophilic nitrogen gave the same intermediate **65**. Eventually, option **C** has the vinyl azide, itself, nucleophilically opening cyclopropane **61** to give intermediate **66**.<sup>34</sup>

In 2018, Cui *et al.* synthesized diverse 2-arylindole **68** derivatives with the Pd(II)-catalyzed cyclization of anilines with vinyl azides **1** (Scheme 24).<sup>35</sup> Indoles are a key structural unit in a large number of synthetic drugs and are widely found in natural products.<sup>36</sup> Indole and its derivatives can also be used in the field of skeletal modification. In this study, the research group developed a palladium-catalyzed highly regioselective cyclization reaction of vinyl azide and aniline by utilizing pyridine as a directing group to produce 2-arylindole derivatives in poor to very good yields (40–84%).<sup>35</sup>

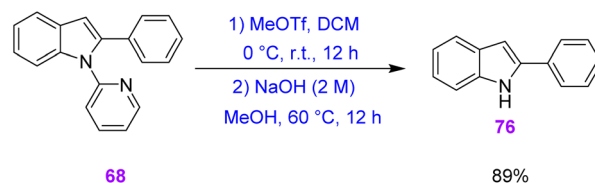
To explain the plausible mechanism of this reaction, a chelation-assisted C–H bond activation first took place *via* a concerted metalation–deprotonation process to generate the six-membered cyclopalladated intermediate **69**. In the next step, two pathways were probably involved in the following transformation. (1) Palladacycle **69** underwent migratory insertion with vinyl azide, and then release of TFA from **73** gave intermediate **74**. Then, oxidative cyclization generated indoline intermediate **75**, which transformed to product **68** *via* the elimination of  $\text{HN}_3$ . Meantime, the catalytically active Pd(II) was regenerated by oxidation of Pd(0). Decomposition of vinyl azide gave 2*H*-azirine **12** by the acceleration of DABCO, which underwent migratory insertion into palladacycle **69** to generate intermediate **70**. In the next step, reductive elimination of **70** produced intermediate **71** with simultaneous formation of Pd(0), which could be reoxidized to the active catalytic Pd(II). In the final step, an intramolecular nucleophilic addition of intermediate **71** resulted in intermediate **72**, which underwent further deamination, generating product **68** (Scheme 25).<sup>35</sup>

Finally, they removed the 2-pyridyl directing group from compound **68**. 2-Arylindole **68** was treated with methyl trifluoromethanesulfonate (MeOTf) to generate a pyridinium intermediate and NH-free indole **76** in 89% yield (Scheme 26).<sup>35</sup>

In 2008, Narasaka *et al.* reached various derivatives of poly-substituted N–H pyrroles through the reaction of vinyl azides and 1,3-dicarbonyl compounds. They proposed two synthetic methods for the synthesis of tetra- and tri-substituted N–H pyrroles that resulted in the production of scaffolds of **80** with good to excellent yields (74–96%) and scaffolds of **81** in poor to



Scheme 25 Mechanism for the synthesis of 2-arylindole **68** through the Pd-catalyzed reaction of vinyl azides **1**.

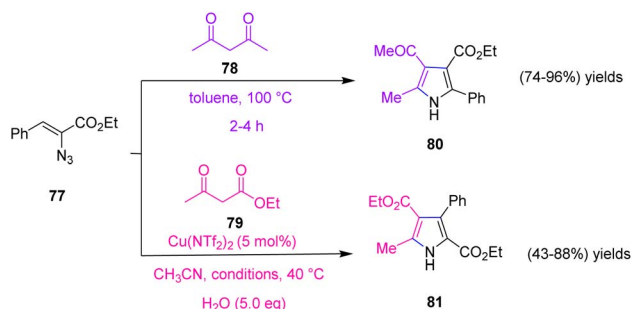


Scheme 26 Removal of the *N*-pyridine group from **68**.

very good yields (43–88%). In method (I) they used the reaction of vinyl azide **77** with 1,3-dicarbonyl **78** compounds that proceed through 1,2-addition of 1,3-dicarbonyl compounds to 2*H*-azirine, the research group used Cu(II)-catalyzed synthesis of pyrroles from vinyl azide **77** and ethyl acetoacetate **79** *via* the 1,4-addition reaction (Scheme 27).<sup>37</sup>

In method (I) they designed a plan to use vinyl azides **77** as precursors of 2*H*-azirines. When a mixture of vinyl azides **77** and acetylacetone **78** was heated in toluene at 85–100 °C (depending on its derivatives), substituted pyrrole was obtained in good to excellent yields (74–96%) (Scheme 28).<sup>37</sup>

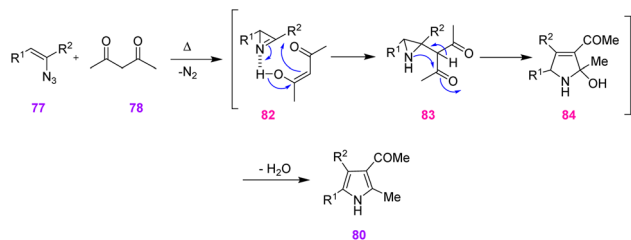
In method (II) since the Cu-catalytic reaction was done at 40–60 °C, it was improbable that a 2*H*-azirine intermediate would be found in the reaction course. The reaction may be started by the 1,4-addition of copper enolate **85** to vinyl azide **77**, the internal nitrogen of which is coordinated to copper. Simultaneous removal of dinitrogen obtained alkylidene amino copper



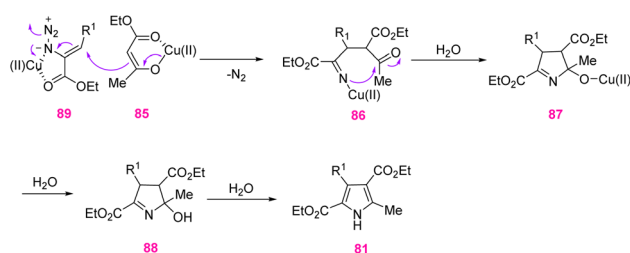
Scheme 27 Synthesis of poly-substituted N–H pyrroles **80** and **81** from vinyl azides **77**.







Scheme 28 Synthesis of pyrroles **80** and **81** from vinyl azides **77** and 1,3-dicarbonyl compounds **78** in toluene.

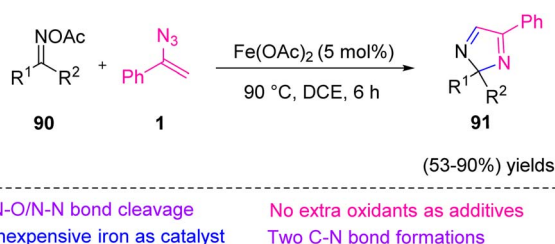


Scheme 29 Mechanism for the Cu-catalyzed synthesis of substituted pyrrole **81** from vinyl azide **77**.

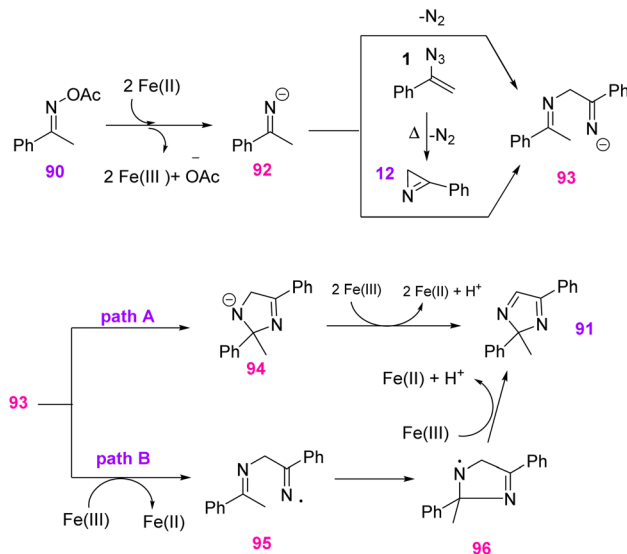
**86** that underwent intramolecular nucleophilic attack on the carbonyl group, producing pyrrole with the extrusion of water (Scheme 29).<sup>37</sup>

In 2017, Jiang *et al.* proposed an approach to produce 2*H*-imidazoles **91** from oxime acetates **90** and vinyl azides **1** under redox-neutral conditions (Scheme 30). They developed a novel method for the synthesis of 2*H*-imidazoles *via* iron-catalyzed [3 + 2]-annulation of oxime acetates with vinyl azides that resulted in a synthesis of scaffolds of **91** in fair to excellent yields (53–90%).<sup>38</sup> 2*H*-Imidazoles are significant motifs found in a broad range of natural products<sup>39</sup> as well as in organic synthesis. These compounds are used for detection of diradical intermediates<sup>40</sup> and could also be used as a chiral auxiliary for organic synthesis reactions.<sup>41</sup> Oximes and their derivatives can be prepared by the reaction of hydroxylamine hydrochloride, ketone, and acetic anhydride.<sup>38</sup>

To explain the possible mechanism, imine anion intermediate **92** was first generated through the reduction of oxime acetate **90** by Fe(II) with a two-step, single-electron-transfer operation. Then, nucleophilic attack may happen between



Scheme 30 Iron-catalyzed reaction of vinyl azides and oxime derivatives **90**.



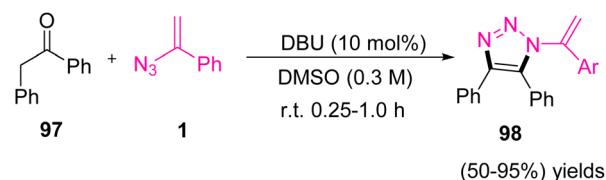
Scheme 31 Mechanism for the iron-catalyzed reaction of vinyl azides and oxime derivatives **90**.

anion intermediate **92** and 2*H*-azirine or the Michael addition–elimination of **92** to vinyl azides **1** to generate intermediate **93**. After that, intermediate **94** was generated through intramolecular cyclization of **93**. Eventually, oxidative dehydrogenation of **94** by Fe(III) generated product **91** (path A). There was another approach in which intermediate **93** was first oxidized by Fe(III) to generate imine radical intermediate **95**, which cyclized to intermediate **96**. In the final step, the desired product was obtained *via* a sequential oxidation deprotonation process (path B) (Scheme 31).<sup>38</sup>

In 2017, Ramachary *et al.* reported the synthesis of fully decorated *N*-vinyl-1,2,3-triazoles **98** scaffolds in good to excellent yields (50–95%) through an organocatalytic vinyl azide–carbonyl [3 + 2]-cycloaddition.<sup>42</sup> Triazoles have an important role in pharmaceutical chemistry and their drug properties mainly depend on their aromatic or aliphatic substitution.<sup>43</sup> Tazobactam, solithromycin, cefatrizine, and rifinamide are some examples of 1,2,3-triazole-based drugs (Scheme 32).<sup>44</sup>

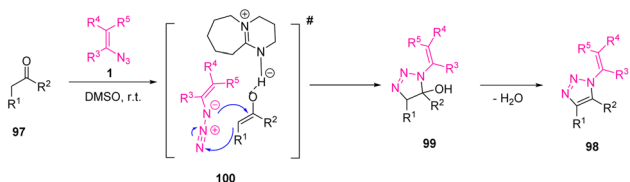
Reaction of the aryl aldehydes/aryl acetones/deoxybenzoines with catalyst DBU in DMSO (solvent) gave the stable enolate that on *in situ* treatment with vinyl azides **1** produced 1,2,3-triazolines by [3 + 2]-cycloaddition (Scheme 33).<sup>42</sup>

In 2017, Tang *et al.* synthesized *N*<sup>2</sup>-substituted 1,2,3-triazoles **102** through copper(I)-mediated carbo-amination of vinyl azides

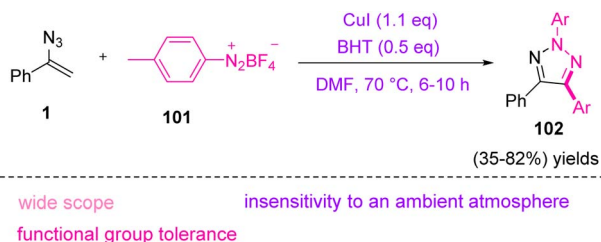


Scheme 32 Synthesis of *N*-vinyl-1,2,3-triazole **98** from vinyl azides **1**.





Scheme 33 Mechanism for the synthesis of *N*-vinyl-1,2,3-triazole **98** from vinyl azides **1**.

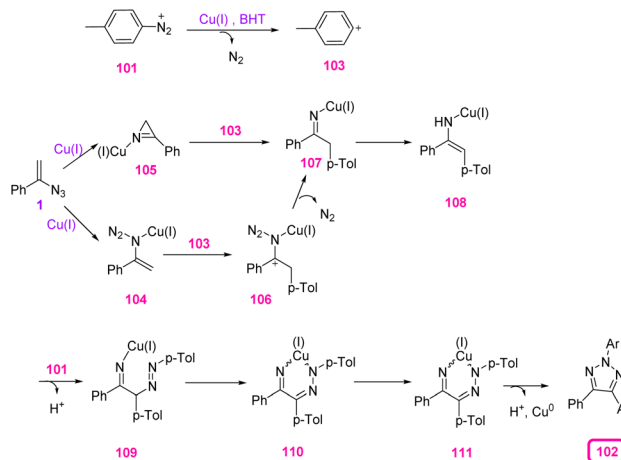


Scheme 34 Copper-catalyzed synthesis of *N*<sup>2</sup>-substituted 1,2,3-triazole **102**.

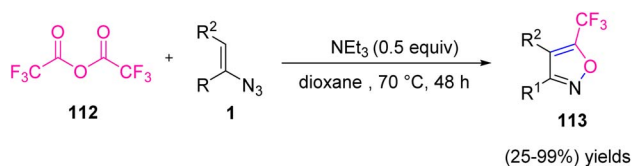
**1** by aryldiazonium salts **101** (Scheme 34). By this strategy, Tang and coworkers succeeded in the synthesis of diverse *N*<sup>2</sup>-substituted 1,2,3-triazoles in poor to very good yields (35–82%).<sup>45</sup> 1,2,3-Triazoles have played an important role in material science, pharmacological development, and chemical biology due to their privileged chemical structures and properties as five-membered heterocycles. 1,2,3-Triazoles have also received interest as chelates,<sup>46</sup> auxiliaries for C–H activation,<sup>47</sup> and systematic carbene precursors.

To illustrate the mechanism of this reaction, the aryl cation **103** was first delivered from aryldiazonium cation **101** with the release of nitrogen under acidic conditions. Copper-chelated complex **104** that was generated from vinyl azides **1** was attacked by aryl cation **103** to generate iminyl metal ions **106**, which could further generate iminyl copper(i) intermediate **107** with the release of dinitrogen. Then, C–N bond cleavage of **105** that was produced from the decomposition of vinyl azide with the aid of Cu(i) generated intermediate **107** in the presence of aryl cation **103**. Then, tautomerization of **107** gave enamide intermediate **108**, which underwent addition with aryldiazonium cation **101** to generate complex **109**. Copper-chelate complex **109** could isomerize to give intermediate **110**. Direct reductive elimination of intermediate **109** produced desired product **102** (Scheme 35).<sup>45</sup>

In 2020, Weng *et al.* developed a novel approach for the synthesis of poly-substituted 5-trifluoromethyl isoxazole **113** and its derivatives (Scheme 36). The research group, through denitrogenative cyclization of vinyl azides with trifluoroacetic anhydride, synthesized diverse 5-trifluoromethyl isoxazoles in poor to quantitative yields (25–99%).<sup>48</sup> Nitrogen- and oxygen-containing heterocycles, due to the exhibition of biological and pharmaceutical activities, such as antimicrobial, antibiotic, anti-inflammatory, and anticancer activities have been receiving a lot of attention in the past few years.<sup>49,50</sup>

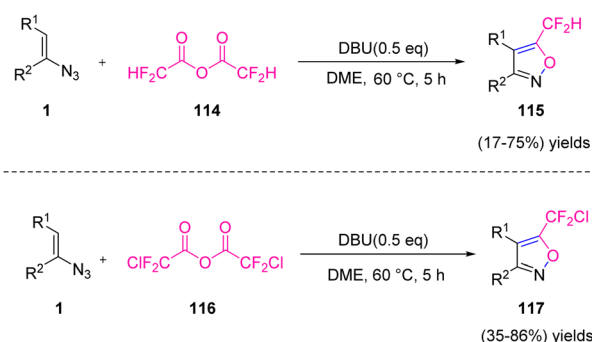


Scheme 35 Mechanism for the copper-catalyzed synthesis of *N*<sup>2</sup>-substituted 1,2,3-triazole **102**.

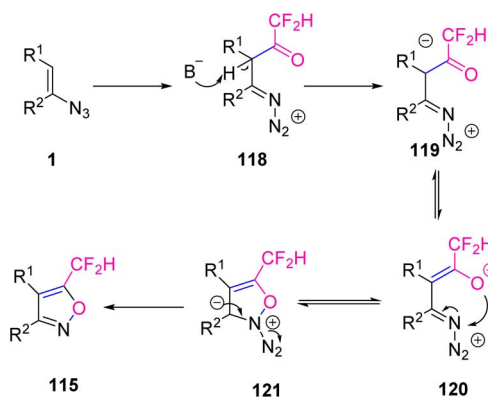


Scheme 36 Synthesis of poly-substituted 5-trifluoromethyl isoxazole **113**.

In the same year, Weng *et al.* synthesized 5-difluoromethyl isoxazoles **115** and 5-chlorodifluoromethyl isoxazole **117** via the reaction between vinyl azides **1** and difluoroacetic anhydride **114** or chlorodifluoroacetic anhydride **116** (Scheme 37). Their method involved sequential difluoroacetylation of vinyl azide, followed by deprotonation, cyclization, and dinitrogen elimination, providing a suitable synthesis of 5-difluoromethyl in poor to good yields (19–75%) and 5-chlorodifluoromethyl isoxazole in poor to very good yields (35–86%).<sup>51</sup> Among organofluorine molecules, difluoromethylated compounds, especially difluoromethylated heterocyclic structures, play a significant and unique role in agricultural and medicinal chemistry.<sup>52</sup> Difluoromethyl (–CF<sub>2</sub>H) behaves in an isopolar and isosteric



Scheme 37 Synthesis of 5-difluoromethyl isoxazoles **115** and 5-chlorodifluoromethyl isoxazole **117**.



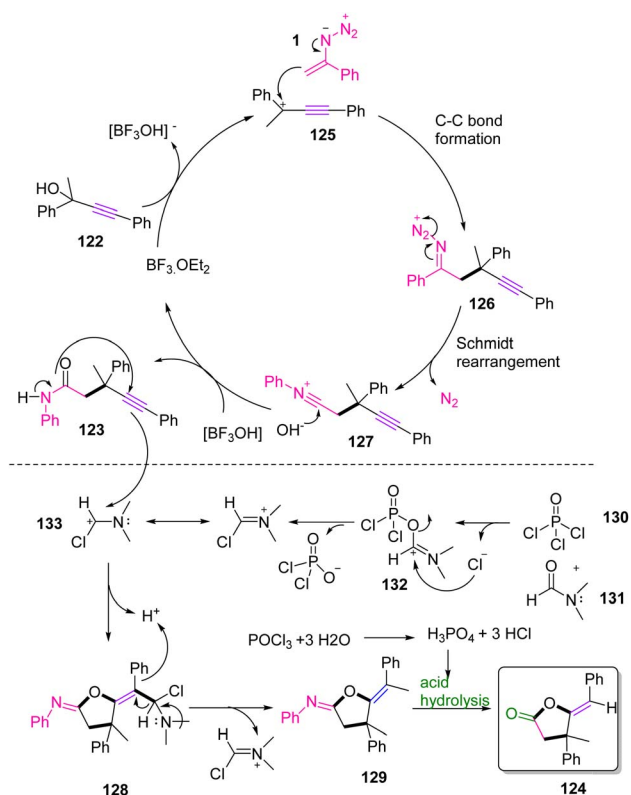
Scheme 38 Mechanism for the synthesis of 5-difluoromethyl isoxazoles **115**.

way to the hydroxyl (–OH) group and can act as a hydrogen donor *via* hydrogen bonding.<sup>53</sup>

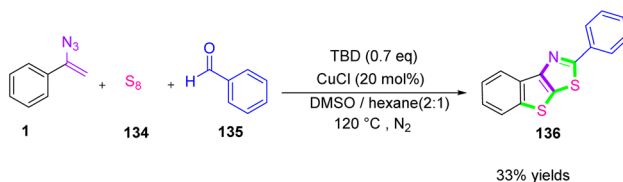
In Scheme 38, difluoroacetylation of vinyl azides **1** with difluoroacetic anhydride **114** first generated intermediate **118**, which underwent deprotonation with a base to give intermediate **119**. Isomerization of **119** to an alkoxy anion **120** followed by a 5-endo cyclization gave intermediate **121**. In a final step, intermediate **121** underwent a dinitrogen elimination to produce desired product **115**.<sup>51</sup>

In 2015, Bi *et al.* introduced a new strategy to synthesize dihydrofuran-2(3*H*)-ones **124** *via* the synthesis of 4-ynamides **123** (Scheme 39). The nucleophilic addition of vinyl azides **1** to propargylic alcohols **122** in the presence of  $\text{BF}_3 \cdot \text{Et}_2\text{O}$  catalysis is an efficient method that produced 4-ynamides in fair to excellent yields (62–90%). Then, a Vilsmeier intramolecular cyclization of 4-ynamides **123** resulted in good to very good yields (73–84%) of dihydrofuran-2(3*H*)-ones **124**, which was the first report of the conversion of alkyne to dihydrofurane-2(3*H*)-ones by the use of a Vilsmeier reagent.<sup>54</sup>

In a plausible mechanism, electrophilic attack of  $\text{BF}_3 \cdot \text{H}_2\text{O}$  on the –OH group of propargylic alcohol **122** first facilitated the generation of propargylic carbocation intermediate **125**, which stimulated the nucleophilic addition of vinyl azides **1** to generate intermediate **126**. Then, intermediate **126** underwent Schmidt rearrangement to give nitrilium intermediate **127**. After that, nitrilium intermediate **127** extracted –OH from  $[\text{BF}_3\text{OH}]^-$  and rearranged to the final product. The Vilsmeier reagent helping intramolecular cyclization involves the production of a Vilsmeier species from the Vilsmeier reagent. Then, the nucleophilic attack of 4-ynamide **123** on Vilsmeier species occurred. Releasing the Vilsmeier species by



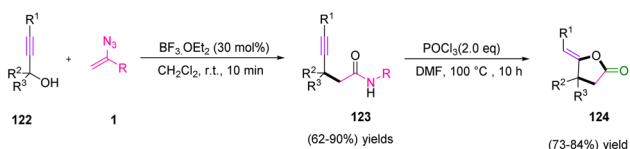
Scheme 40 Mechanism for the synthesis of dihydrofuran-2(3*H*)-ones **124** by using vinyl azides **1**.



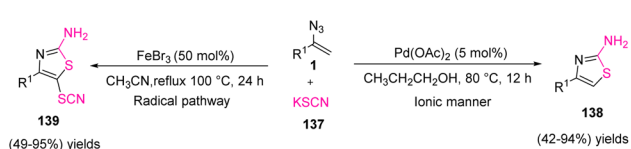
Scheme 41 Copper-catalyzed synthesis of bis-S-heterocycles **136**.

displacement with a proton produced **129** and eventually hydrolytic cleavage of **129** afforded final product **124** (Scheme 40).<sup>54</sup>

In 2019, Jiang *et al.* synthesized bis-S-heterocycles **136** *via* copper-catalyzed three-component tandem cyclization by the use of  $\text{S}_8$  **134** as a sulfur source (Scheme 41). In this protocol, the research team used  $\text{S}_8$  as two sulfur atom donors for thiophene and thiazole rings, respectively. Organic sulfides are an important class of compound that have been broadly used in

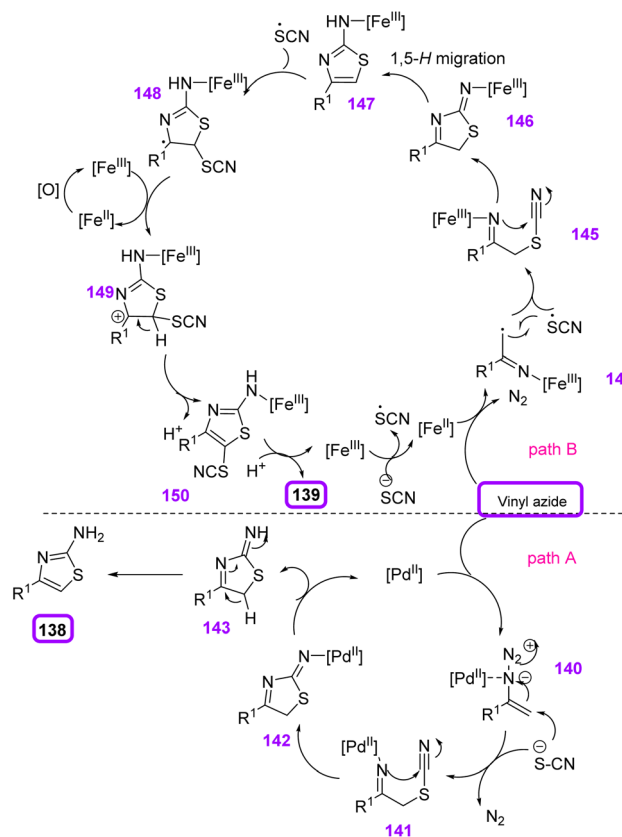


Scheme 39 Synthesis of dihydrofuran-2(3*H*)-ones **124** by using vinyl azides.



Scheme 42 Iron- and palladium-catalyzed reaction of vinyl azides and potassium thiocyanate **137**.





**Scheme 43** Mechanism for iron- and palladium-catalyzed reaction of vinyl azides **1** and potassium thiocyanate **137**.

biomedical fields. In recent years, many drugs that are listed as best-selling drugs contain sulfur.<sup>55</sup>

For example, cefmenoxime,<sup>56</sup> a bis-*S*-heterocyclic, is an antibiotic with a high curative effect on special kinds of bacteria, and nocodazole,<sup>57</sup> a thiophene structure, is an anti-cancer drug that can inhibit cancer cell division.

The research team in this work employed a concise synthetic mode to pick up the thiophene and thiazole ring in a one-pot method, in which  $S_8$  was utilized as a two-sulfur donor.<sup>55</sup>

In 2015, Yu *et al.* reported selective access to 4-substituted 2-aminothiazoles **138** and 4-substituted 5-thiocyano-2-aminothiazoles **139** from potassium thiocyanate **137** and vinyl azides **1** switched by palladium and iron catalysts (Scheme 42). Yu and co-workers constructed diverse derivatives of 4-substituted 2-aminothiazoles in poor to excellent yields (42–94%) and 5-thiocyano-2-aminothiazoles in poor to excellent yields (49–95%).<sup>58</sup> 2-Aminothiazoles and their derivatives are one of the most significant aza-heterocycles broadly found in pharmaceutical compounds and natural products. The wide spectrum of biological activities shown by this structure include antimicrobial,<sup>59</sup> anticancer,<sup>60</sup> antiviral and antiprion, and anti-inflammatory effects. The most widely utilized synthetic method to gain 2-aminothiazoles is the Hantzsch cyclocondensation of thiourea and  $\alpha$ -halo carbonyl compounds.<sup>61</sup> Many other methods to synthesize 2-aminothiazoles have also been expanded.<sup>58</sup>

For the  $Pd(OAc)_2$ -catalyzed reaction (path A), the first coordination of palladium(II) to the azide group gave palladium(II)-azide complex **140**, expanding the electrophilicity of pendant

**Table 1** Synthesis of five-membered heterocycles through vinyl azides

| Catalyst (mol%)                                 | Solvent              | Temperature    | MW irradiation | Yields | Reference               |
|---|----------------------|----------------|----------------|--------|-------------------------|
| $Cu(OAc)_2$ (10 mol%)                           | DMF                  | 40 °C          | ✗              | 50–93% | Donthiri <sup>13</sup>  |
| CuNPs (30 mol%)                                 | DCE                  | 135 °C         | ✗              | 50–83% | Jiang <sup>17</sup>     |
| Eosin Y (3 mol%)                                | $CH_3CN$             | r.t.           | ✓              | 57–97% | Liu <sup>20</sup>       |
| Eosin Y (3 mol%)                                | $CH_3CN$             | r.t.           | ✗              | 57–97% |                         |
| $Cu(OAc)_2$ (5 mol%)                            |                      |                |                |        |                         |
| $NiCl_2 \cdot glyme$ (5 mol%)                   | 1,4-Dioxane          | 70 °C          | ✗              | 56–77% | Guo <sup>24</sup>       |
| $Rh[CodCl]_2$ (2.5 mol%)                        | 1,4-Dioxane          | r.t. to 120 °C | ✗              | 16–96% | Zhang <sup>25</sup>     |
| DPPE (5 mol%)                                   |                      |                |                |        |                         |
| CuI (10 mol%)                                   | Acetonitrile         | 65 °C          | ✗              | 48–76% | Bairagi <sup>28</sup>   |
| $NiCl_2$ (5 mol%)                               | DAMc                 | 110 °C         | ✗              | 40–82% | Jiao <sup>31</sup>      |
| $Cu(OAc)_2$ (4 mol%)                            | DMSO/EtOH            | 110 °C         | ✗              | 39–79% |                         |
| $Dy(OTf)_3$ (10 mol%)                           | Toluene              | 110 °C         | ✗              | 25–92% | Kerr <sup>34</sup>      |
| $Pd(TFA)$ (10 mol%)                             | Toluene              | 75 °C          | ✗              | 40–84% | Cui <sup>35</sup>       |
| No cat.   | Toluene              | 100 °C         | ✗              | 74–96% | Narasaka <sup>37</sup>  |
| $Cu(NTf_2)_2$ (5 mol%)                          | Acetonitrile/ $H_2O$ | 40 °C          | ✗              | 43–88% |                         |
| $Fe(OAc)_2$ (5 mol%)                            | DCE                  | 90 °C          | ✗              | 53–90% | Jiang <sup>38</sup>     |
| DBU (10 mol%)                                   | DMSO                 | r.t.           | ✗              | 53–95% | Ramachary <sup>42</sup> |
| Taking advantage of non-catalytic amount of CuI | DMF                  | 70 °C          | ✗              | 35–82% | Tang <sup>45</sup>      |
| No cat.   | Dioxane              | 70 °C          | ✗              | 25–99% | Weng <sup>48</sup>      |
| No cat.   | DME                  | 60 °C          | ✗              | 17–75% | Weng <sup>51</sup>      |
| No cat.   | DME                  | 60 °C          | ✗              | 35–86% |                         |
| $BF_3 \cdot OEt_2$ (30 mol%)                    | $CH_2Cl_2$           | r.t.           | ✗              | 62–90% | Bi <sup>54</sup>        |
| CuI (20 mol%)                                   | DMSO/hexene          | 120 °C         | ✗              | 33%    | Jiang <sup>55</sup>     |
| $Pd(OAc)_2$ (5 mol%)                            | $CH_3CH_2CH_2OH$     | 80 °C          | ✗              | 42–94% | Yu <sup>58</sup>        |
| $FeBr_3$ (50 mol%)                              | $CH_3CN$             | 80 °C          | ✗              | 49–95% |                         |





olefin. The nucleophilic attack of potassium thiocyanate sent  $N_2$  out to give intermediate **141**, and its intramolecular nucleophilic attack on the cyano group generated intermediate **142**. Protonation of intermediate **142** and then aromatization would produce 4-substituted 2-aminothiazoles **138**. But for the  $FeBr_3$ -catalyzed reaction, one-electron oxidation of the thiocyanate anion by iron(III) bromide first generated a thiocyanate radical with the release of reduced iron(II) species. Vinyl azide was reduced by iron(II) to provide an iminyl iron(III) radical with the removal of molecular nitrogen. Thiocyanate radicals added to radical **144** to generate alkylidenamino iron(III) **145**, which underwent an intramolecular nucleophilic assault to give intermediate **146**. Then, 1,5-*H* migration of **146** gave 2-aminothiazole intermediate **147**, which can be converted to 4-substituted 2-aminothiazoles *via* protonation. Thiocyanate radicals attacked the electron-rich site of 2-aminothiazole **147** to generate radical **148**, which was oxidized by iron(III) to generate cation **149**. Deprotonation of cation **149** gave the target 4-substituted 5-thiocyano-2-aminothiazoles **139** with the regeneration of iron(III) (Scheme 43).<sup>58</sup>

Table 1 was prepared to provide a summary of the strategies the research groups utilized to synthesize five-membered heterocycle derivatives in which the catalyst, solvent, temperature, yields, and MW irradiation are compared.

## Formation of 6-membered heterocycles

In 2018, Guo *et al.* approached a great method to synthesize substituted phenanthridines **153** (Scheme 44). Guo's research group, by using metal-free, visible-light-promoted decarboxylative radical cyclization of *N*-acryloxy phthalimides **152** and vinyl azides **151** synthesized diverse phenanthridines in poor to very good yields (32–80%).<sup>62</sup> Phenanthridines are in a significant class of alkaloids that show remarkable biological activities and optoelectronic properties, so many efforts have been devoted to developing efficient strategies for the synthesis of these motifs.<sup>63</sup>

Photoexcitation of eosin Y by visible light generated excited eosin  $Y^*$ . Oxidative quenching of eosin  $Y^*$  by single electron transfer (SET) to an NHP ester gave radical anion **154** along with eosin  $Y^{+}$ . A phthalimide anion and the corresponding alkyl radical **155**, were generated through fragmentation of  $CO_2$  from **154**. Then, the phthalimide anion and alkyl radical **155** added to

the C=C bond of **152**, furnishing iminyl radical **156** by releasing  $N_2$ . Iminyl radical **156** underwent an intramolecular cyclization to give intermediate **157**, which was oxidized by eosin  $Y^{+}$  to generate the corresponding carbocation **158**. In the last step, deprotonation of intermediate **158** gave the desired product **153** (Scheme 45).<sup>62</sup>

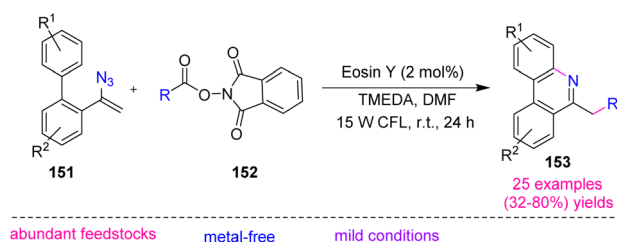
In 2021, Wang *et al.* reported a novel method to synthesize 2,4-diaryl-6-trifluoromethylated pyridines **160** through copper-catalyzed cyclization of  $CF_3$ -ynones **159** and vinyl azides **1** (Scheme 46). Their procedure for this transformation led to the production of diverse 2,4-diaryl-6-trifluoromethylated pyridines in poor to fair yields (36–65%).<sup>64</sup> Pyridine derivatives are versatile precursors of different topoisomerase I inhibitors and anticancer agents.<sup>65</sup> The pyridine skeletons containing trifluoromethyl motifs, like 2-trifluoromethylated pyridines, have emerged as core units in an increasing number of important agrochemicals and drugs.<sup>66</sup>

To explain the mechanism of Wang and coworkers' methods, the reaction of vinyl azides **1** with  $PPh_3$  first gave vinyl iminophosphorane **161** through the Staudinger–Meyer reaction. Then, **161** was trapped by electrophilic  $CF_3$ -ynone through copper-accelerated 1,4-addition to give intermediate **162**, which would further give intermediate **163** and the corresponding resonance **164** while  $PPh_3$  and  $H_2O$  were present in the reaction system. Finally, 2,4-diaryl-6-trifluoromethylpyridine **160** was generated through cascade intramolecular cyclization and dehydration processes with the assistance of PMEDTA (path A). Meanwhile, 1,2-addition from intermediate **161** and  $CF_3$ -ynone **159** could proceed as well to form the iminophosphorane **166**, which further delivered intermediate **167** and the corresponding resonance **168**. Then, intramolecular hydroamination on the alkyne moiety resulted in cyclic intermediate **168** with the aid of  $Cu(II)$  species, and dehydration gave 2,6-diaryl-4-trifluoromethylpyridine compound **170** (path B) (Scheme 47).<sup>64</sup>

In 2019, Guo *et al.* proposed a new method by utilizing cycloketone oxime esters **24** and vinyl azides **1** to produce substituted phenanthridines **172** (Scheme 48). This reaction proceeded under mild and redox-neutral conditions with a wide substrate scope that resulted in the synthesis of diverse phenanthridines in fair to very good yields (63–81%).<sup>24</sup>

In the plausible mechanism, Ni-mediated single-electron reduction of cyclobutanone oxime ester first generated iminyl radical **26**, which underwent C–C bond cleavage producing cyanoalkyl radical **27**. In the next step, radical **27**, added to the C=C bond of vinyl azide, generated iminyl radical **28** by releasing  $N_2$ . For biaryl vinyl azides, iminyl radical **28** underwent oxidative cyclization to afford the final product **172** (Scheme 49).<sup>24</sup>

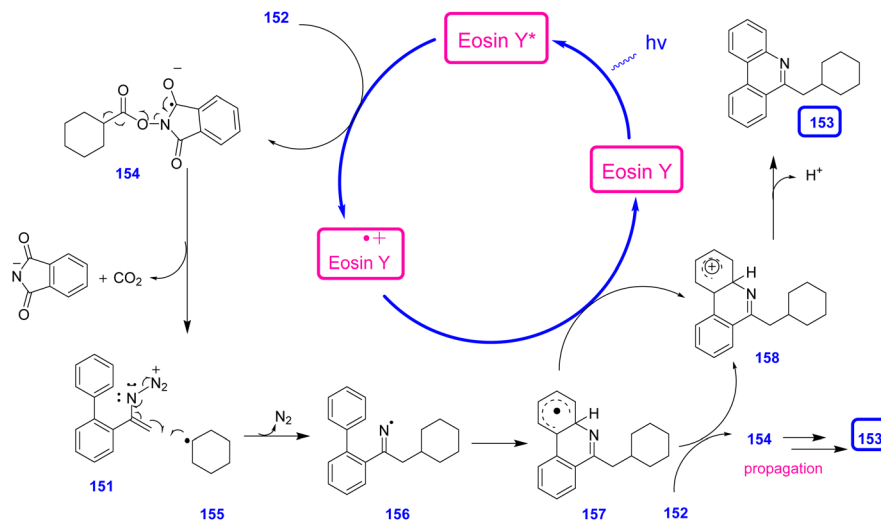
In 2016, Jiang *et al.* attempted to synthesize isoquinoline derivatives **176** and **177** *via* palladium-catalyzed C–H functionalization of aromatic oxime **175** (Scheme 50). With this strategy, through the  $Pd(II)$ -catalyzed cyclization reaction of aromatic oxime **175** and vinyl azides **1**, they synthesized diverse isoquinolines in poor to very good yields (25–85%). Oximes are fascinating building blocks in synthetic chemistry because of their easy preparation, efficient reactivity, and harmless byproducts.<sup>67</sup>



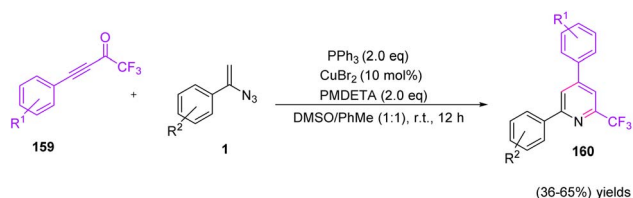
**Scheme 44** Synthesis of substituted phenanthridines **153** through the reaction of *N*-acryloxy **152** phthalimides and vinyl azides **151**.







Scheme 45 Mechanism for the synthesis of substituted phenanthridines **153** through the reaction of *N*-acryloxy phthalimides and vinyl azides **151**.

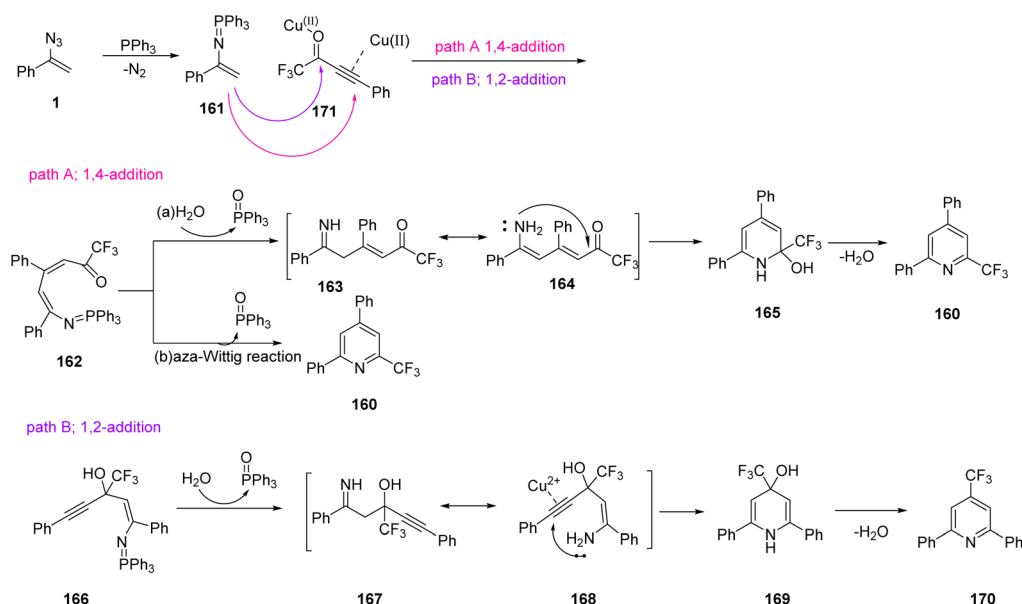


Scheme 46 Copper-catalyzed synthesis of 2,4-diaryl-6-trifluoromethylated pyridines **160**.

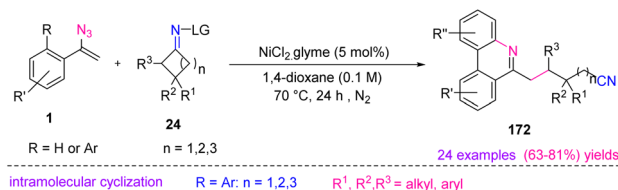
In the possible mechanism, an oxime directing group *ortho*-C–H bond cleavage by Pd(II) first took place to form palladacycle intermediate **178**. The thermal decomposition of vinyl azides **1**

occurred to generate 2*H*-azirines that underwent migratory insertion into palladacycle **178** to generate intermediate **179**. After that, the reductive elimination of **179** gave intermediate **180** and released the Pd species, that underwent further oxidative addition across the C–N bond to prepare imido-Pd species **181**. Intramolecular condensation of **181** regenerated Pd(II) and gave **182** that concomitantly released hydroxylamine to form product **176** (Scheme 51).<sup>67</sup>

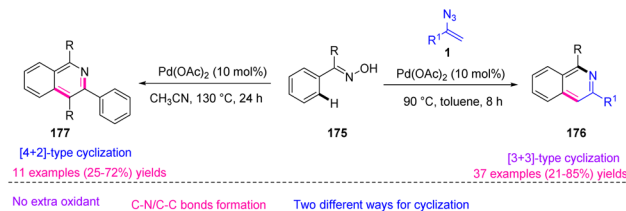
In 2018, Zhou *et al.* found a one-pot approach to obtain derivatives of 6-(sulfonylmethyl) phenanthridines **184** (Scheme 52). They used visible-light-induced sulfonylation/cyclization of vinyl azides **151** and developed a strategy to synthesize 6-(sulfonylmethyl)-phenanthridines **184** in poor to excellent



Scheme 47 Mechanism for the copper-catalyzed synthesis of 2,4-diaryl-6-trifluoromethylated pyridines **160**.



**Scheme 48** Nickel-catalyzed reaction of cycloketone oxime esters **24** and vinyl azides **1**.



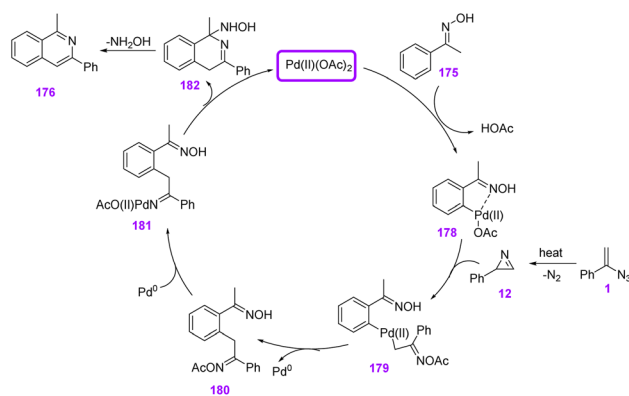
**Scheme 50** Palladium-catalyzed synthesis of isoquinoline derivatives **176** and **177**.

yields (26–93%). Zhou's research group also utilized readily available sulfonyl chloride **183** as a sulfonylation reagent.<sup>68</sup>

In 2016, Liu *et al.* synthesized diverse trifluoromethyl isoquinolines **187** by utilizing multicomponent cascade synthesis from alkynes **186** and vinyl azides **1** (Scheme 53). The research group used Togni's reagent **185** as a CF<sub>3</sub> radical supplier; they also used the Rh(III)–Cu(II) bimetallic system for their methods that resulted in the production of trifluoromethyl isoquinolines in poor to very good yields (21–85%).<sup>69</sup> The trifluoromethyl group is highly important among fluorine functional groups because of its remarkable potential for modulating a molecule's chemical, physical, and biochemical properties.<sup>70</sup> Togni's reagent has been utilized to produce trifluoromethylate compounds, usually in the presence of Cu salts as catalysts.<sup>69</sup>

The mechanism of this reaction was proposed as depicted in Scheme 54. In step 1, CF<sub>3</sub> radicals may first be generated from Togni's reagent in the presence of Cu(II). The CF<sub>3</sub> radical may be added to vinyl azides **1** to generate hypothetical radical intermediate **188**, which could then be trapped by Cu(II) to generate **189** (step 2). Intermediate **189** would react with Rh(III) through an iminyl rhodium intermediate **190** to give rhodacyclic intermediate **191**. Insertion of alkyne **186** generated intermediate **192**, which underwent reductive elimination to produce **187**, along with the Rh(I) species. In the final step, a redox reaction between Rh(I) and Cu(III) regenerated the Rh(III) species.<sup>69</sup>

In 2022, Jiang *et al.* proposed an approach to produce alicyclic[*b*]-fused pyridine **194** via C(sp<sup>2</sup>)-H activation of  $\alpha,\beta$ -unsaturated *N*-acetyl hydrazones **193** with vinyl azides **1** (Scheme 55). This strategy resulted in the production of diverse

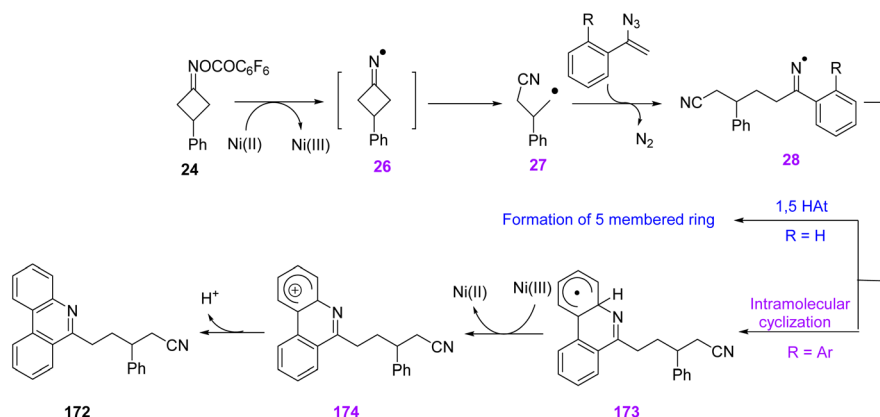


**Scheme 51** Mechanism for palladium-catalyzed synthesis of isoquinoline derivatives **176**.

alicyclic[*b*]-fused pyridines in poor to very good yields (23–80%). Alicyclic[*b*]-fused pyridine scaffolds exist everywhere in natural products, functional materials, ligands, and pharmaceuticals. For example, tacrine that contains a cyclohexane[*b*]-fused pyridine structural skeleton has shown remedial potential in Alzheimer's disease.

Various substance scopes and specific regioselectivities were shown in this reaction. As regards the broad application of alicyclic[*b*]-fused pyridine, it is expected this Pd-catalyzed regioselective C–H activation will gain wide synthetic usage.<sup>71</sup>

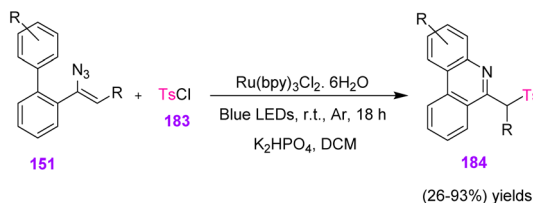
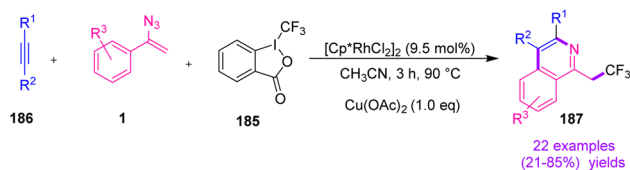
In the plausible mechanism of the reaction, Pd(II)-catalyzed C–H activation with  $\alpha,\beta$ -unsaturated hydrazone first formed



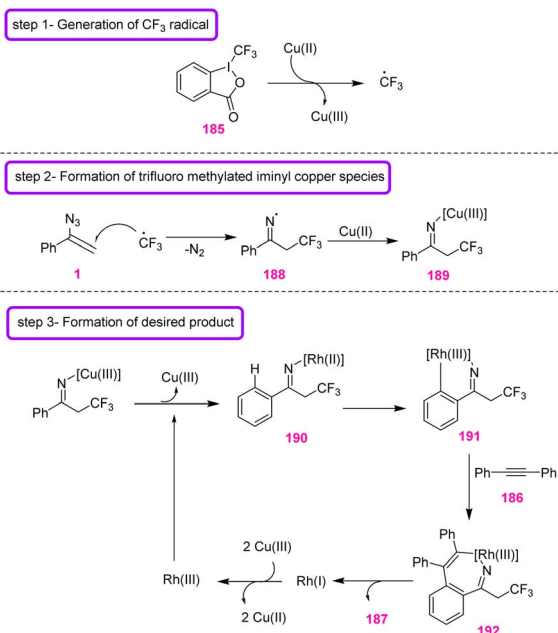
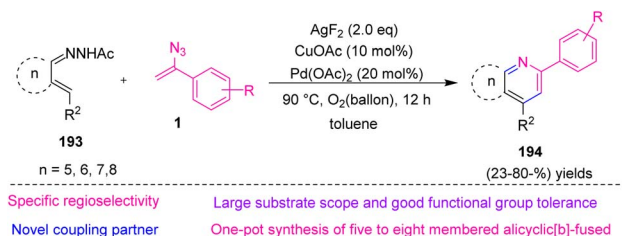
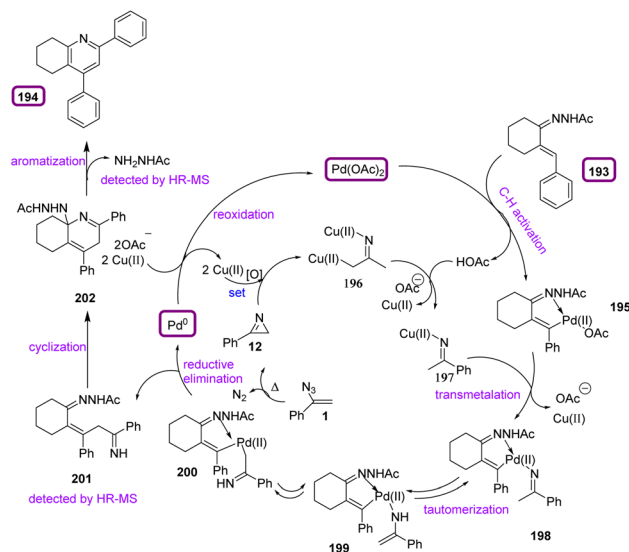
**Scheme 49** Mechanism for the nickel-catalyzed reaction of cycloketone oxime esters **24** and vinyl azides **1**.



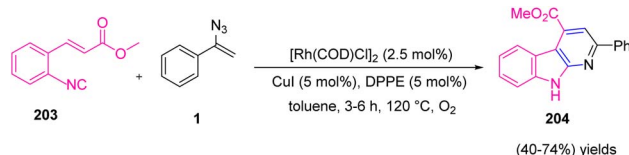
## Review

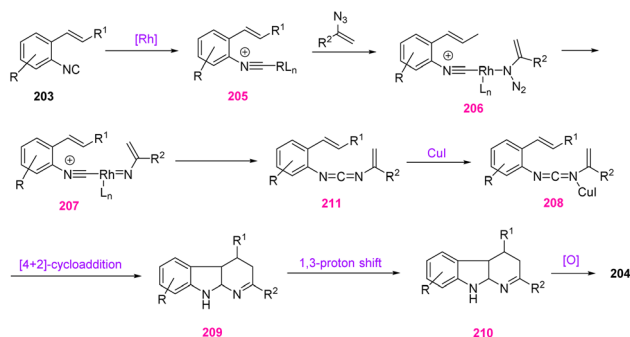
Scheme 52 Synthesis of 6-(sulfonylmethyl) phenanthridines **184**.Scheme 53 Rhodium-catalyzed synthesis of trifluoromethyl isoquinolines **187**.

intermediate **195**, along with the release of HOAc. Pyrolysis of vinyl azides **1** generated 2*H*-azirines which underwent C–N bond cleavage and reduction with Cu(I) to yield Cu(II) aza-enolate **196** species. Next, protonation with HOAc gave iminyl copper species **197**. Also, *trans*-metalation with intermediate **195** generated iminyl palladium species **198**, which underwent tautomerization to form Pd(II) complex **199**. Afterward, the reductive elimination of **200** provided intermediate **201** and Pd(0) species. The Pd(II) catalyst was reproduced through reoxidation with Pd(0) by the Ag/Cu oxidant. Then, intramolecular condensation and subsequent aromatization with the release of  $\text{NH}_2\text{NHAc}$  produced the pyridine product **194** (Scheme 56).<sup>71</sup>

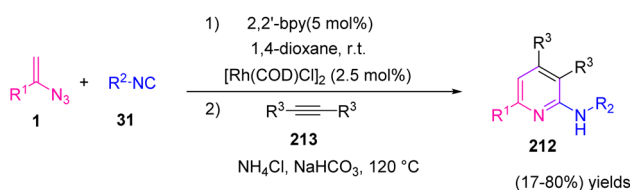
Scheme 54 Plausible mechanism for the synthesis of trifluoromethyl isoquinoline **187**.Scheme 55 Palladium-catalyzed synthesis of alicyclic[b]-fused pyridine **194** via  $\text{C}(\text{sp}^2)\text{--H}$  activation.Scheme 56 Mechanism for the palladium-catalyzed synthesis of alicyclic[b]-fused pyridine **194** via  $\text{C}(\text{sp}^2)\text{--H}$  activation.

In 2020, Zhao *et al.* reported a one-pot and novel method to obtain  $\alpha$ -carbolines **204** through rhodium/copper-catalyzed coupling-cyclization of *O*-alkenyl aryl isocyanides **203** with vinyl azides **1** (Scheme 57). In this method, the reactive vinyl carbodiimides, produced *in situ* from the coupling reaction of vinyl azides **1** with *O*-alkenyl aryl isocyanides **203**, underwent intermolecular [4 + 2]-cycloaddition and provided a new method for the synthesis of poly-substituted  $\alpha$ -carbolines in poor to excellent yields (40–74%). Among different functionalized aryl isocyanides, *O*-alkenyl aryl isocyanides have appeared as valuable precursors for the efficient synthesis of different fused azaheterocycles in the past decade.<sup>72</sup>

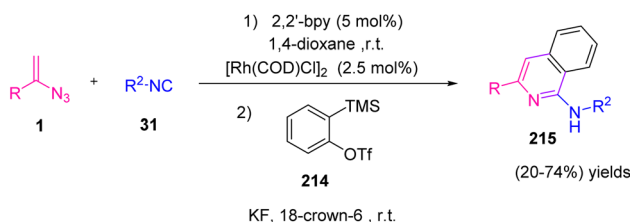
Scheme 57 Rhodium/copper-catalyzed coupling-cyclization of *O*-alkenyl aryl isocyanides **203** with vinyl azides.



Scheme 58 Mechanism for rhodium/copper-catalyzed coupling-cyclization of *O*-alkenyl aryl isocyanides with vinyl azides.



Scheme 59 Rhodium-catalyzed synthesis of pyridine derivatives **212** by utilizing vinyl azides and isonitrile.

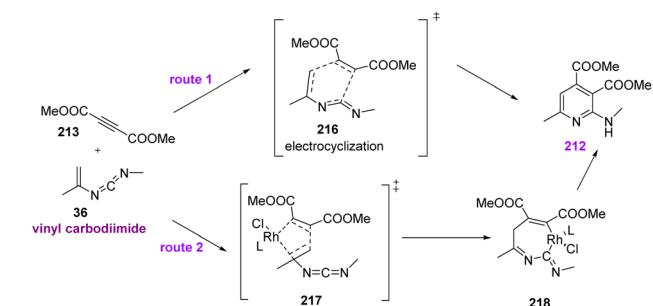


Scheme 60 Formation of aminoisoquinoline **215** through the reaction of vinyl azides and isonitrile.

The proposed mechanism of this reaction is depicted in Scheme 58. First, aryl isocyanide **203** coordinated with  $[\text{Cp}^*\text{RhCl}_2]_2$  to generate intermediate **205**, which coordinated with vinyl azides **1** to give **206**. Then, intermediate **206** released  $\text{N}_2$  to give nitrene intermediate **207**, which underwent migratory insertion, and rhodium was released to produce vinyl carbodiimide **211**. In the next step, intermediate **208**, which was activated by copper, underwent an intermolecular  $[4 + 2]$ -cycloaddition to give intermediate **209**. In the last step,  $\alpha$ -carbolines **204** were produced through a  $1,3$ -*H* shift and oxidative aromatization process.<sup>72</sup>

In 2018, Zhang *et al.* developed a new and efficient method by utilizing vinyl azides **1**, isocyanides **31**, and alkynes **213** in the presence of Rh as catalyst to synthesize various derivatives of pyridine and isoquinoline in poor to very good yields (17–80%) (Scheme 59).<sup>4</sup>

The cascade cyclization was further developed from alkynes to benzynes **214**, which afforded aminoisoquinoline **215** as the product in poor to good yields (20–74%) (Scheme 60).<sup>4</sup>

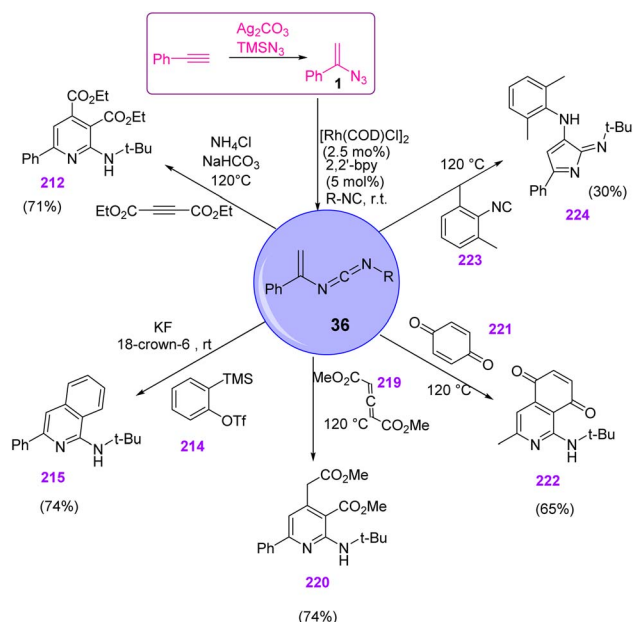


Scheme 61 Mechanism for the rhodium-catalyzed synthesis of substituted pyridine **212**.

After the generation of vinyl carbodiimide **36**, from the reaction of vinyl azides **1** and isocyanide **31** two pathways were possible: direct electrocyclic cyclization or  $\text{Rh}(\text{I})$ -catalyzed oxidative/cyclization/reductive elimination (Scheme 61).<sup>4</sup>

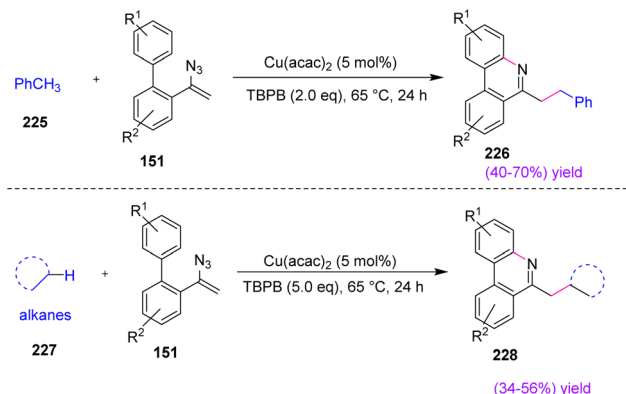
This research group also used vinyl carbodiimides for the synthesis of different heterocycles. Other popular cyclic building blocks were employed to construct different aza-heterocycles. When vinyl carbodiimide reacted with an allene **219**, aminopyridine **220** was obtained in 74% yield. The reaction of vinyl carbodiimide with benzoquinone **221** led to the formation of aminoisoquinoline-5,8-dione **222** in 65% yield. The vinyl carbodiimide intermediate **36** could also go through an  $\alpha,\alpha$ -insertion reaction with another isocyanide to produce pyrrole-2-imine **224** with 30% yield (Scheme 62).<sup>4</sup>

In 2016, Gua *et al.* synthesized substituted phenanthridines **226** and **228** through the copper-catalyzed oxidative cyclization of vinyl azides **151** with the benzylic  $\text{C}_{\text{sp}^3}\text{H}$  bond in poor to good yields (40–70%) and (34–56%) (Scheme 63).<sup>73</sup> Toluene **225** and its derivatives are important chemical starting materials



Scheme 62 Vinyl carbodiimides **36** for the synthesis of other heterocycles.



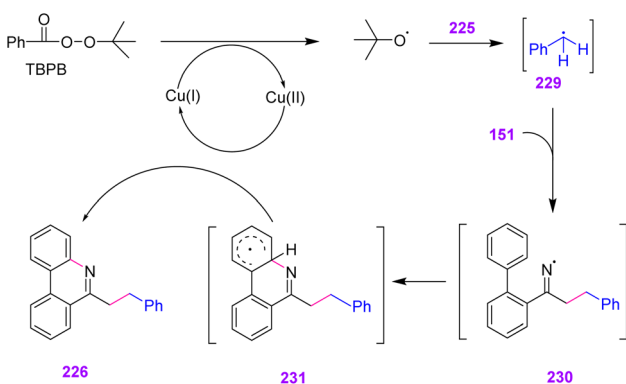


Scheme 63 Synthesis of substituted phenanthridines **226** and **228** through the copper-catalyzed oxidative cyclization of vinyl azides.

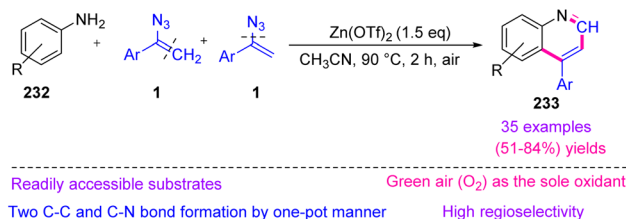
that are widely utilized as solvents in organic synthesis and the chemical industry.<sup>74</sup> Phenanthridines are an important class of alkaloids that, due to their remarkable biological activities and optoelectronic properties, have attracted the interest of chemists. The research group, in this protocol, presented a cyclization process involving the capture of an iminyl radical by the intramolecular aryl ring, which provided a distinctive idea for constructing the phenanthridine framework.<sup>73</sup>

To illustrate the mechanism, metal-mediated single electron transfer (SET) or thermal homolytic cleavage or oxidation of TBPB first yielded the *tert*-butoxy radical. Subsequent hydrogen abstraction from toluene by the *tert*-butoxy radical created benzyl radical **290**. Then, radical **230** added to the double bond of vinyl azide, producing an iminyl radical with the release of dinitrogen. After that, radical **230** underwent an intramolecular cyclization to create radical **231**, which was converted to the corresponding carbocation by Cu(II) via single-electron oxidation with subsequent loss of H<sup>+</sup>, regenerating Cu(I) and producing desired product **226** (Scheme 64).<sup>73</sup>

In 2018, Jiang *et al.* synthesized 4-substituted quinolines **233** with vinyl azides **1** as dual synthons through C–N and C=C bond cleavage in fair to very good yields (51–84%). In this



Scheme 64 Mechanism for the synthesis of substituted phenanthridines **226** through copper-catalyzed oxidative cyclization of vinyl azides.



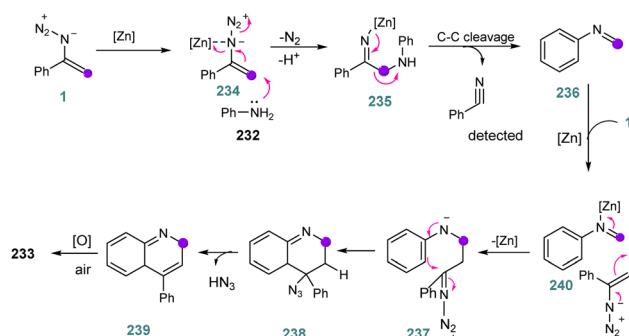
Scheme 65 Vinyl azides as dual synthons for the synthesis of 4-substituted quinolines **233**.

protocol, vinyl azides acted as dual synthons through C=C and C–N bond cleavage with the formation of two C=C bonds and one C=N bond (Scheme 65).<sup>2</sup> As a new strategy to further develop MCRs, the dual-synthon approach, which uses one reactant to obtain multiple fragments, has attracted a lot of attention.<sup>75</sup>

The mechanism of this reaction can be seen in Scheme 66. First, intermediate **234** was generated by the coordination of zinc to the azide, enhancing the electrophilicity of the olefin. Then, a nucleophilic attack by the aniline produced intermediate **235**. After that, intermediate **235** generated imine intermediate **236** through C–C bond cleavage. In the next step, intermediate **236** underwent an intramolecular cyclization with vinyl azides **1** to generate intermediate **238**. Intermediate **238** converted to **239** with the elimination of HN<sub>3</sub>. Eventually, aromatization of **239** by O<sub>2</sub> in air obtained desired product **233**.<sup>2</sup>

In 2009, Wang *et al.* developed a new method to synthesize diverse substituted pyridines **242** in poor to very good yields (11–84%) and 2-azabicyclo[3,3,1]non-2-en-1-ols **244** in poor to excellent yields (28–91%). This study focused on the use of cyclopropanols **241** as precursors of β-carbonyl radicals and reactions of vinyl azides. In this protocol, utilization of Mn(acac)<sub>3</sub> was found to be essential because it might play a dual role in the oxidation of cyclopropanol and dihydropyridine **250** (Scheme 67).<sup>76</sup>

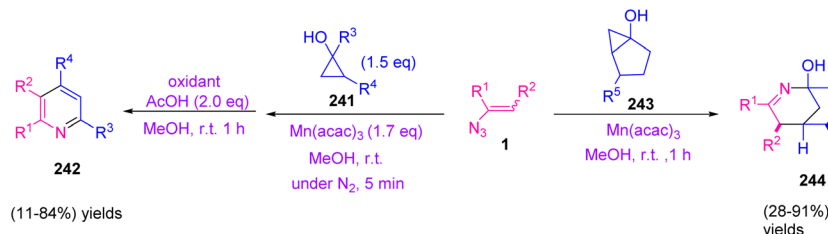
The reaction was initiated by the addition of β-keto radical **245**, which was produced by one-electron oxidation of **241** by Mn(III) to vinyl azide, generating iminyl radical **246** with the release of dinitrogen. Cyclization of iminyl radical **246** to an intramolecular carbonyl group would generate alkoxy radical



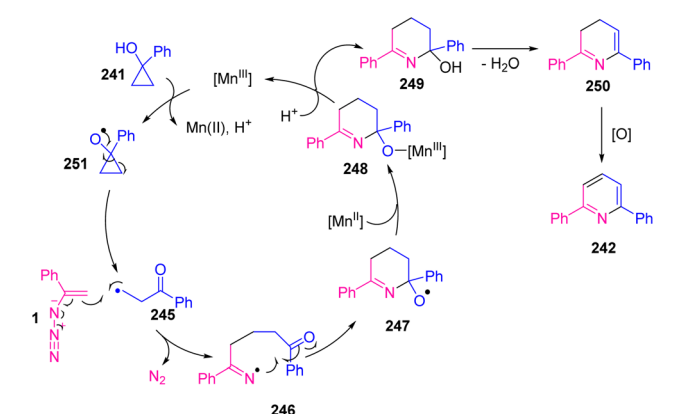
Scheme 66 Mechanism for the synthesis of 4-substituted quinolines **233**.







Scheme 67 Synthesis of substituted pyridines **242** and 2-azabicyclo[3,3,1]non-2-en-1-ols **244** via vinyl azides **1**.



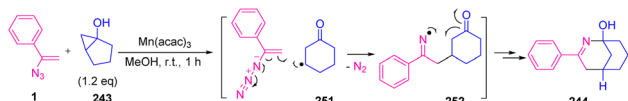
Scheme 68 Mechanism for the synthesis of substituted pyridines **242** via vinyl azides **1**.

**247** that can be reduced by Mn(II) and then protonated to give tetrahydropyridine **249**. Dehydration of **249** and further oxidation producing dihydropyridine **250** would produce desired pyridine **242** (Scheme 68).<sup>76</sup>

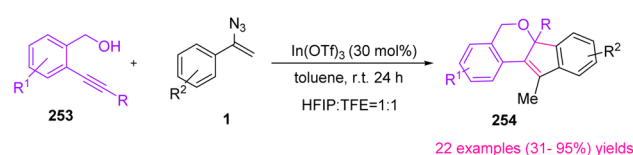
Treatment of chiral bicyclic cyclopropanol **243** with vinyl azides **1** provided racemic **244**. Generation of ring-expanded  $\beta$ -keto radical **251** from bicyclic cyclopropanol followed by radical addition of **251** to vinyl azides **1** was probable in the reaction mechanism (Scheme 69).<sup>76</sup>

In 2015, Liu *et al.* utilized Lewis-acid-catalyzed polycyclization of internal alkynols **253** and vinyl azides **1** to synthesize pyran-based indeno[1,2-*c*]isochromene **254** scaffolds (Scheme 70). With this strategy, the research group synthesized 22 examples of this compound in poor to excellent yields (31–95%).<sup>77</sup> Tetrahydropyran rings are common in a wide array of biologically and pharmacologically relevant natural products. In Fig. 6 some examples of natural products containing octahydrocyclopenta[*b*]pyran motif are shown.<sup>78</sup>

Initially, the triple bond of **253** coordinated with In(OTf)<sub>3</sub>, promoting the electrophilicity of the alkyne. Then, the hydroxyl



Scheme 69 Mechanism for the synthesis of 2-azabicyclo[3,3,1]non-2-en-1-ols **244** via vinyl azides **1**.



Scheme 70 Synthesis of pyran-based indeno[1,2-*c*]isochromene scaffolds via vinyl azides.

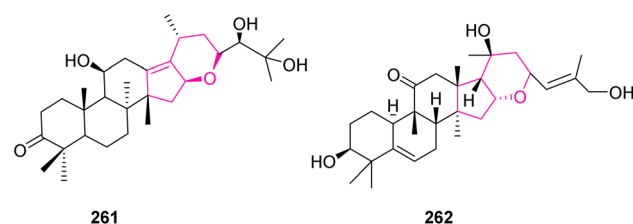
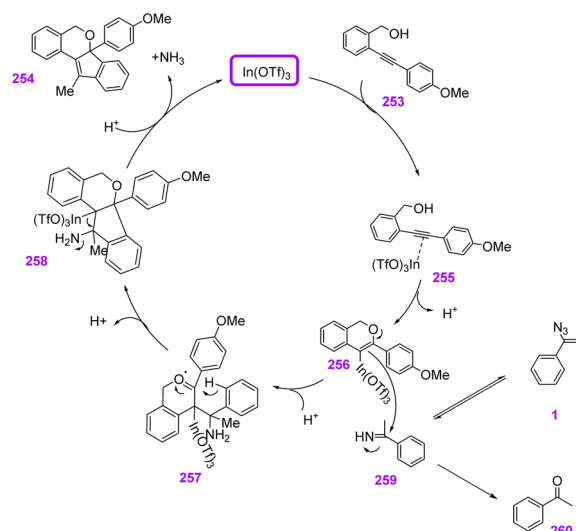


Fig. 6 Examples of natural products containing an octahydrocyclopenta[*b*]pyran motif.

group added to the electron-deficient alkyne, giving vinyl-indium species **256**. After that, **256** was trapped by the *N*-unsubstituted imine, which gave intermediate **257**. Then, carbocyclization of **257** generated **258**. Acid-promoted cleavage of



Scheme 71 Mechanism for the synthesis of pyran-based indeno[1,2-*c*]isochromene **254** scaffolds via vinyl azides.



Table 2 Synthesis of six-membered heterocycles through vinyl azides

| Catalyst (mol%)   | Solvent            | Temperature | MW irradiation | Yields | Reference           |
|---|--------------------|-------------|----------------|--------|---------------------|
| Eosin Y (2 mol%)  | DMF                | r.t.        | ✓              | 32–80% | Guo <sup>62</sup>   |
| CuBr <sub>2</sub> (10 mol%)                                       | DMSO/PhMe          | r.t.        | ✗              | 36–65% | Wang <sup>64</sup>  |
| NiCl <sub>2</sub> ·glyme (5 mol%)                                 | 1,4-Dioxane        | 70 °C       | ✗              | 63–81% | Guo <sup>24</sup>   |
| Pd(OAc) <sub>2</sub> (10 mol%)                                    | Toluene            | 90 °C       | ✗              | 25–85% | Jiang <sup>67</sup> |
| Ru(bpy) <sub>3</sub> Cl <sub>2</sub> ·H <sub>2</sub> O (2 mol%)   | DCM                | r.t.        | ✓              | 26–93% | Zhou <sup>68</sup>  |
| [CP*RhCl <sub>2</sub> ] <sub>2</sub> (9.5 mol%)                   | CH <sub>3</sub> CN | 90 °C       | ✗              | 21–85% | Liu <sup>69</sup>   |
| Pd(OAc) <sub>2</sub> (20 mol%)                                    | Toluene            | 90 °C       | ✗              | 23–80% | Jiang <sup>71</sup> |
| Cu(OAc) (10 mol%)   |                    |             |                |        |                     |
| [Rh(COD)Cl] <sub>2</sub> (2.5 mol%) CuI (5 mol%)                  | Toluene            | 120 °C      | ✗              | 40–74% | Zhao <sup>72</sup>  |
| [Rh(COD)Cl] <sub>2</sub> (2.5 mol%)                               | 1,4-Dioxane        | r.t.        | ✗              | 17–80% | Zhang <sup>4</sup>  |
| Cu(acac) <sub>3</sub> (5 mol%)                                    | Toluene            | 65 °C       | ✗              | 40–70% | Gua <sup>73</sup>   |
| Taking advantage of non-catalytic amount of Zn (OTf) <sub>2</sub> | CH <sub>3</sub> CN | 90 °C       | ✗              | 51–84% | Jiang <sup>2</sup>  |
| Taking advantage of non-catalytic amount of Mn(acac) <sub>3</sub> | MeOH               | r.t.        | ✗              | 33–84% | Wang <sup>76</sup>  |
| Mn(acac) <sub>3</sub> (5 mol%)                                    | MeOH               | r.t.        | ✗              | 28–91% |                     |
| In(OTf) <sub>3</sub> (30 mol%)                                    | Toluene            | r.t.        | ✗              | 31–95% | Liu <sup>77</sup>   |

the carbon–metal bond, and elimination led to final product **254** (Scheme 71).<sup>77</sup>

Table 2 provides a summary of the strategies the researchers utilized to synthesize six-membered heterocycles derivatives in which the catalyst, solvent, temperature, yields, and MW irradiation have been compared.

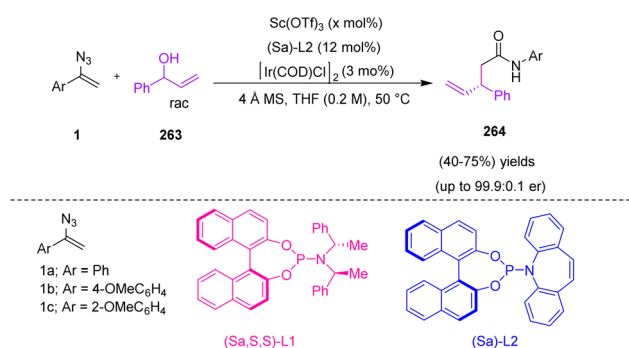
## Others

In 2020, Mukherjee *et al.* developed an efficient method for the enantioselective  $\alpha$ -alkylation of amides using vinyl azides **1** as an enolate surrogate (Scheme 72). By this strategy, Mukherjee and coworkers succeeded in synthesizing derivatives of **264** in poor to good yields (40–75%). Among the unstabilized enolates utilized as nucleophiles in iridium-catalyzed asymmetric allylic alkylation reactions, amide enolates are the least explored. In this study, vinyl azides **1** were employed as amide enolate surrogates in Ir-catalyzed asymmetric allylic alkylation with branched allylic alcohols **263** as the allylic electrophile.<sup>79</sup>

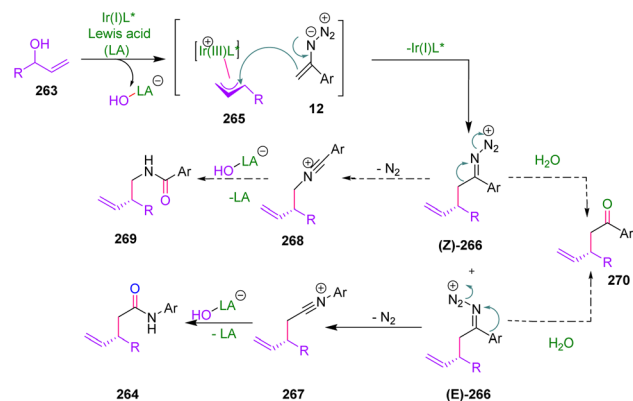
In the possible mechanism, the nucleophilic addition of vinyl azides **1** to the more substituted terminal of an electrophilic  $\pi$ -allyl-Ir complex was expected to give branched imino

diazonium ion **266**, which can generate a mixture of (*E*)- and (*Z*)-isomers. Schmidt-type rearrangement of (*E*)-**266** through 1,2-aryl migration followed by hydration of the resulting nitrilium ion **267** would then furnish the  $\alpha$ -functionalized acetamide **264**. A competitive pathway involving (*Z*)-**266** favored 1,2-alkyl migration to generate an isomeric nitrilium ion **268** and finally *N*-homo-allylbenzamide derivatives **269**. Controlling the geometry of **266** was critical to ensure the desired aryl migration. Another competitive pathway contained the hydrolysis of imino-diazonium ion **266** to the  $\alpha$ -allyl ketone **270**. The suppression of the latter two pathways has been the key to the success of this method (Scheme 73).<sup>79</sup>

In 2021, O. Terent'ev *et al.* reported the photo-redox-catalyzed synthesis of *N*-unsubstituted enamino sulfones **272** from vinyl azides **1** and sulfinates **271** (Scheme 74). The research group used ethanol as solvent and eosin Y as photocatalyst in combination with nitrobenzene as an electron shuttle. In this strategy, elimination of N<sub>2</sub> from vinyl azides allowed the energetically favorable production of enamine derivatives in poor to fair yields (38–68%).<sup>80</sup>



Scheme 72 Enantioselective  $\alpha$ -allylic alkylation (AAA) of amide **264** through vinyl azides **1**.

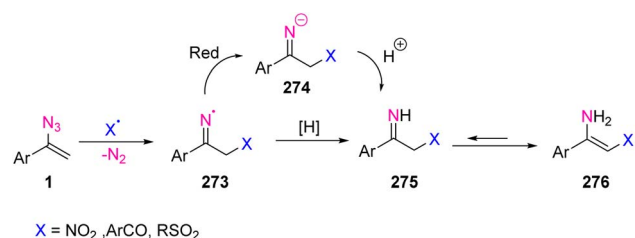


Scheme 73 Mechanism for the enantioselective  $\alpha$ -allylic alkylation (AAA) of amide **264** through vinyl azides **1**.





Scheme 74 Photo-redox-catalyzed synthesis of *N*-unsubstituted enamino sulfones **272** through vinyl azides **1**.



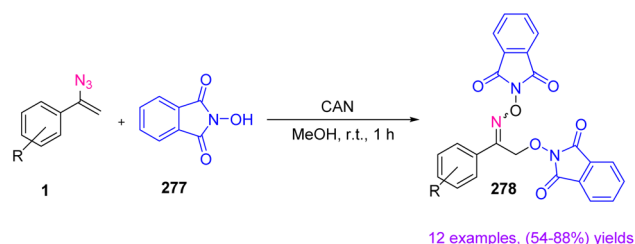
Scheme 75 Radical addition to vinyl azides for the synthesis of *N*-unsubstituted enamine.

Formation of *N*-unsubstituted enamine derivatives through radical addition to vinyl azides **1** is depicted in Scheme 75.<sup>80</sup>

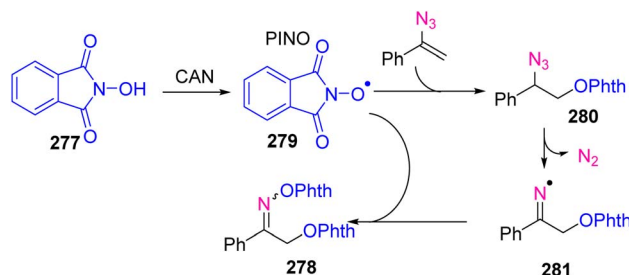
In 2020, O. Terent'ev *et al.* reported a cerium(IV) ammonium nitrate promoted synthesis of *O*-phthalimide oximes **278** from *N*-hydroxy phthalimide **277** and vinyl azides **1** (Scheme 76). The disclosed protocol was based on the radical transformation of vinyl azides with the release of nitrogen and the formation of iminyl *N*-radicals that led to the formation of *O*-phthalimide oximes in fair to very good yields (54–88%).<sup>81</sup> *N*-oxyl radicals are broadly used in biological and organic chemistry and material science.<sup>82</sup> In organic synthesis, more stable nitroxyl radicals are utilized as a catalyst for the oxidation of alcohol and free radical scavengers.<sup>83,84</sup>

The plausible mechanism started with the formation of a PINO radical **279** from NHPI **277** under the action of CAN, followed by addition to the terminal carbon of the C=C bond of vinyl azides **1**. Nitrogen elimination from **280** occurred with the generation of iminyl radical **281**. In the last step, radical **281** was intercepted by the PINO radical to form the final product **278** (Scheme 77).<sup>81</sup>

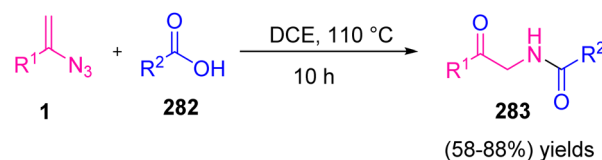
In 2020, Fan *et al.* proposed a new method to synthesize  $\alpha$ -amido ketone **283** through the cascade reaction of carboxylic acid **282** with vinyl azides **1** under catalyst-free conditions



Scheme 76 Synthesis of *O*-phthalimide oximes **278** from *N*-hydroxy phthalimide **277** and vinyl azides **1**.



Scheme 77 Mechanism for the synthesis of *O*-phthalimide oximes **278**.



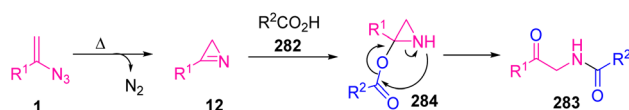
Scheme 78 Synthesis of  $\alpha$ -amido ketones **283** through the reaction of carboxylic acid **282** with vinyl azides **1**.

(Scheme 78). This strategy led to the formation of diverse  $\alpha$ -amido ketones in fair to very good yields (58–88%).<sup>85</sup>  $\alpha$ -Amido ketone derivatives have attracted attention due to their being not only necessary motifs of a plethora of pharmaceutically active compounds but also essential intermediates that are broadly utilized in organic synthesis.<sup>86</sup>

To explain the mechanism, the vinyl azides **1** were first decomposed under the reaction conditions to generate an azirine intermediate **12**. Then, **12** reacted with carboxylic acid **282** to generate an azirine **284**. Eventually, the unstable aziridine **284** through a thermal rearrangement produced  $\alpha$ -amido ketone **283** (Scheme 79).<sup>85</sup>

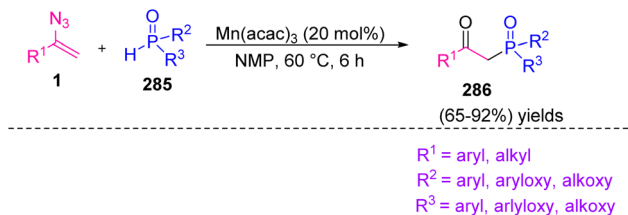
In 2017, Yu *et al.* synthesized  $\beta$ -keto phosphine oxides **286** through Mn(III)-catalyzed phosphorylation of vinyl azides **1** in fair to excellent yields (65–92%).<sup>87</sup> Organophosphorus compounds play an important role in material science, organic chemistry, and pharmaceuticals.<sup>88</sup> In recent years, protocols between organo-phosphorous radicals and radical acceptors have been expanded for producing organo-phosphorous compounds, especially for the production of  $\beta$ -keto phosphine oxides (Scheme 80).<sup>89,90</sup>

The mechanism of this reaction might be initiated by the addition of phosphine radical **288**, produced by one-electron oxidation of **287** by Mn(III) to vinyl azide, generating iminyl radical **289** with the release of N<sub>2</sub>. Sequentially, the produced iminyl radical **289** was reduced by Mn(II) and then protonated to

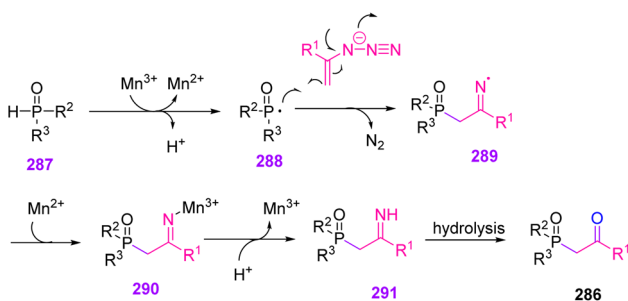


Scheme 79 Mechanism for the synthesis of  $\alpha$ -amido ketones **283** through the reaction of carboxylic acid with vinyl azides.

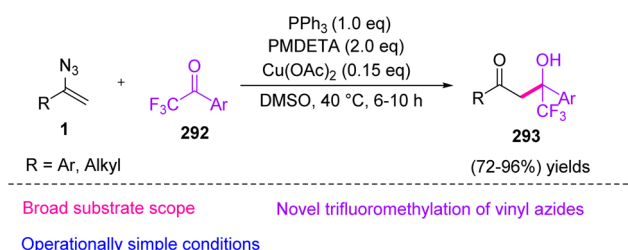




Scheme 80 Mn(III)-catalyzed synthesis of  $\beta$ -keto phosphine oxides **286**.



Scheme 81 Mechanism for the Mn(III)-catalyzed synthesis of  $\beta$ -keto phosphine oxides **286**.



Scheme 82 Copper-catalyzed aldol reaction of vinyl azides with trifluoromethyl ketone **292**.

generate imine intermediate **291**. The hydrolysis of **291** would produce the desired  $\beta$ -keto phosphonate or  $\beta$ -keto phosphine oxides **286** (Scheme 81).<sup>87</sup>

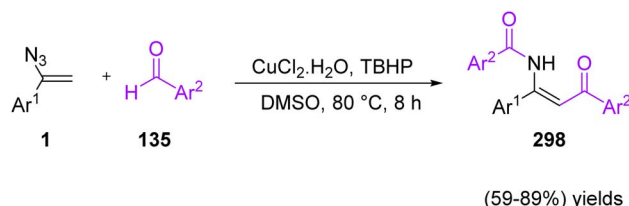
In 2019, Tang *et al.* proposed a new method to synthesize  $\beta$ -hydroxy-trifluoromethyl ketone **293** (Scheme 82) through the copper-catalyzed aldol reaction of vinyl azides **1** with

trifluoromethyl ketone **292** in good to excellent yields (72–96%).<sup>91</sup> The trifluoromethyl group ( $\text{CF}_3$ ) appears to have wide applications in pharmaceuticals, such as mefloquine (antimalaria),<sup>92</sup> efavirenz (anti-HIV),<sup>93</sup> and sorafenib (anti-cancer).<sup>94</sup>

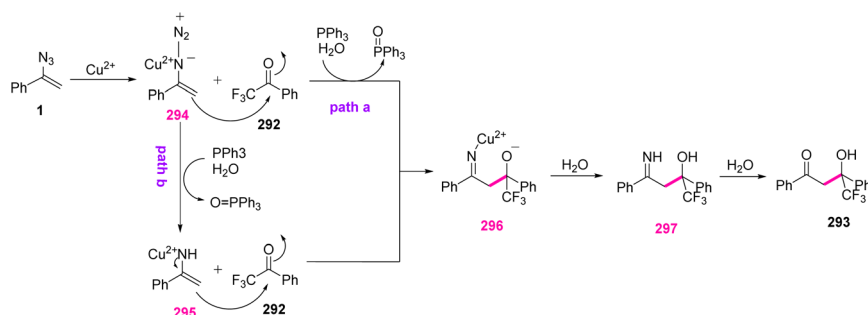
In the possible mechanism, vinyl azides **1** first complexed with  $\text{Cu(II)}$  to give an *N*-diazo enamine copper **294**, which comfortably trapped electrophile **292** by nucleophilic addition to generate intermediate **296** with concomitant release of  $\text{N}_2$  under standard conditions (path a). Another plausible active intermediate **295**, produced from **294** in the presence of  $\text{PPh}_3$  and trace  $\text{H}_2\text{O}$  in the reaction vessel, underwent nucleophilic addition with trifluoromethyl ketone to give intermediate **296** (path b). Protonation of imine copper **296** with  $\text{H}_2\text{O}$  could further afford imine **297**, with the release of a  $\text{Cu}^{2+}$  ion. Eventually, the hydrolysis reaction of **297** produced final product **293** (Scheme 83).<sup>91</sup>

In 2022, Wang *et al.* developed a  $\text{CuCl}_2 \cdot 2\text{H}_2\text{O}$ /TBHP-mediated method for the synthesis of  $\beta$ -enaminones **298** via a coupling reaction of vinyl azides **1** with aldehydes **135** (Scheme 84). By using this protocol, Wang and co-workers succeeded in synthesizing diverse  $\beta$ -enaminones in fair to very good yields (59–89%).<sup>95</sup>  $\beta$ -Enaminones are important pharmaceutically active compounds. They are also versatile and extremely attractive intermediates utilized in the preparation of pharmaceutical targets and various heterocyclic compounds.<sup>96</sup>  $\beta$ -Enaminones are also used as *N,O*-bidentate ligands in transition-metal-catalyzed reactions and organoboron complexes.<sup>97</sup>

The mechanism of this reaction can be seen in Scheme 85. First, TBHP underwent a single electron transfer (SET) to give *t*-BuO $\cdot$  radical and/or *t*-BuOO $\cdot$  radical by the action of copper ions. Then, benzoyl radical **299** was generated *via* the processes

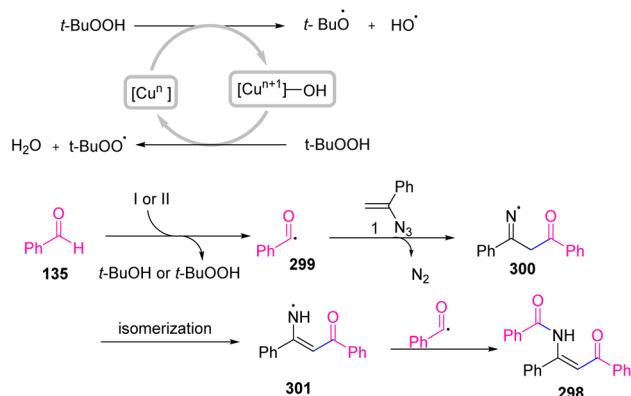


Scheme 84 Synthesis of  $\beta$ -enaminones **298** via a coupling reaction of vinyl azides with aldehydes **135**.



Scheme 83 Mechanism for the copper-catalyzed aldol reaction of vinyl azides with trifluoromethyl ketone **292**.

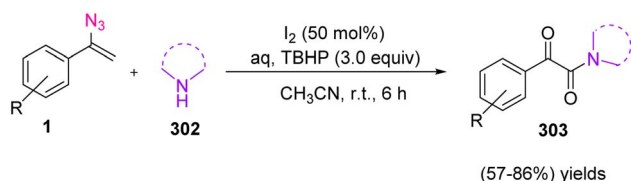




Scheme 85 Mechanism for the synthesis of  $\beta$ -enaminones **298** via a coupling reaction of vinyl azides with aldehydes.

of deprotonation and oxidation of benzaldehyde **135** in the vicinity of the  $t\text{-BuO}^\bullet$  radical and/or  $t\text{-BuOO}^\bullet$  radical, which then attacked the terminal carbon of the  $\text{C}=\text{C}$  bond of  $\alpha$ -phenyl vinyl azide, affording iminyl radical **300** with the release of nitrogen. The generated radical **300** then underwent isomerization to produce enaminyl radical **301**, which recombined with radical **299** to give final product **298**.<sup>95</sup>

In 2022, Dandela *et al.* published the iodine-TBHP mediated synthesis of  $\alpha$ -ketoamide **303** through the reaction of vinyl azides **1** and amines **302** in fair to very good yields (57–86%). This reaction can be seen in Scheme 86.<sup>5</sup>  $\alpha$ -Ketoamides and their derivatives are present in a variety of natural products, biologically active molecules such as antitumor, anti-IBD,<sup>98</sup> antiviral,<sup>99</sup> anti-HIV,<sup>100</sup> and antibacterial drugs, and functional materials. The  $\alpha$ -ketoamide moieties are also present in diverse pharmacologically interesting compounds, as shown in Fig. 7.<sup>5</sup>



Scheme 86 Synthesis of  $\alpha$ -keto thioamide **303** from vinyl azides and amines.

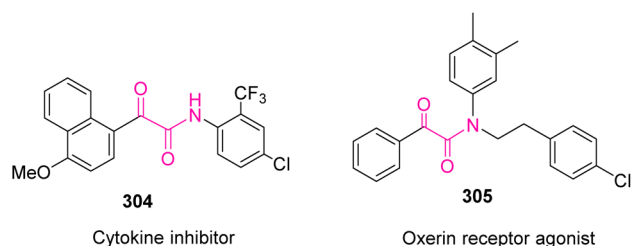
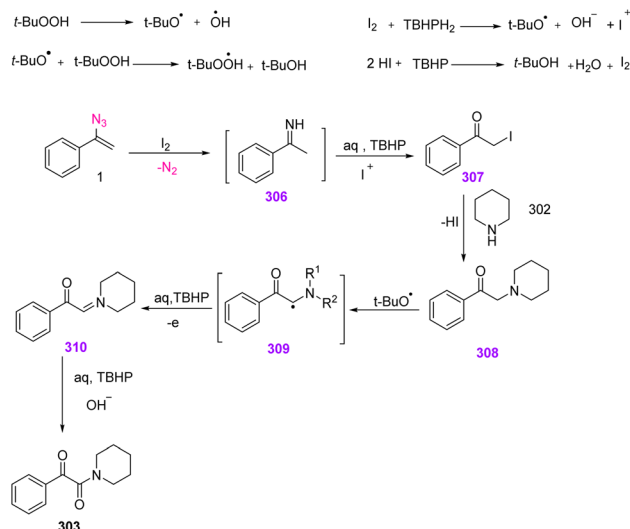


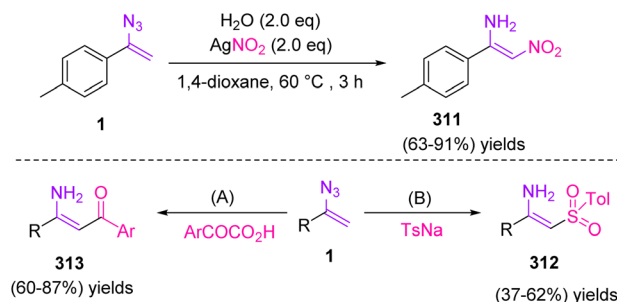
Fig. 7 Examples of biologically active molecules containing  $\alpha$ -ketoamides.



Scheme 87 Mechanism for the synthesis of  $\alpha$ -keto thioamide **303** from vinyl azides **1** and amines.

In the possible mechanism, in the presence of  $\text{I}_2$ ,  $N$ -unsubstituted imine **306** would first be generated from  $\alpha$ -aryl vinyl azides, with the release of  $\text{N}_2$ . Then, aq. TBHP would cause the hydrolysis of imine intermediate **306**. In the next step, iodinated intermediate **307** could be generated. The nucleophilic substitution of amine to intermediate **307** gave  $\alpha$ -aminoketone **308** which was converted to intermediate **309**. In the presence of aq. TBHP **309** converted to intermediate **310**. Eventually, this iminium intermediate oxidized to produce final product **303** (Scheme 87).<sup>5</sup>

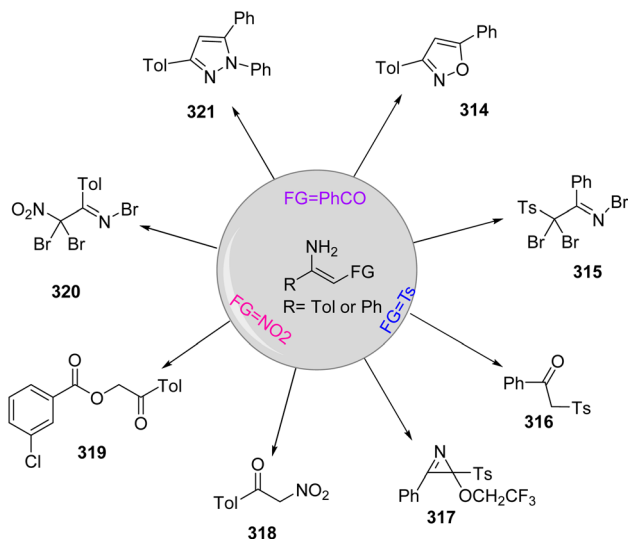
In 2017, Bi *et al.* synthesized  $N$ -unprotected enamines **311**, **312**, and **313** through radical enamination of vinyl azides **1** in fair to excellent yields (63–91%), poor to fair yields (37–62%), and fair to very good yields (60–87%), respectively (Scheme 88). In this work, the research group focused on establishing the relationship between enamines and vinyl azides. It was found that an electron-withdrawing-group-generable radical induced enamination of vinyl azides, which resulted in different types of  $\beta$ -functionalized  $N$ -unprotected enamines. The research team eventually found this goal using acyl, nitro, and sulfonyl radicals, thereby providing a general way to access different types of  $\beta$ -functionalized  $N$ -unprotected enamines.<sup>101</sup>



Scheme 88 Synthesis of  $N$ -unprotected enamines **311**, **312**, and **313**.





Scheme 89 Transformation of  $\beta$ -functionalized enamine.

To evaluate the scalability of this strategy, Bi and coworkers further transformed the  $\beta$ -functionalized primary enamines to many bioactive molecules as useful building blocks according to Scheme 89.<sup>101</sup>

In 2019, Singh *et al.* developed a novel method for the synthesis of 3-oxoisindoline-1-acetamides **323** (Scheme 90). This reaction progressed at ambient temperature with a broad range of 3-hydroxy isindole-1-ones and vinyl azides and resulted in the production of 3-oxoisindoline-1-acetamides in fair to excellent yields (67–97%).<sup>102</sup> In modern pharmaceuticals and biologically active compounds, the amide functionality is omnipresent. It has also been found that small organic molecules containing methylene amide linkages are in many

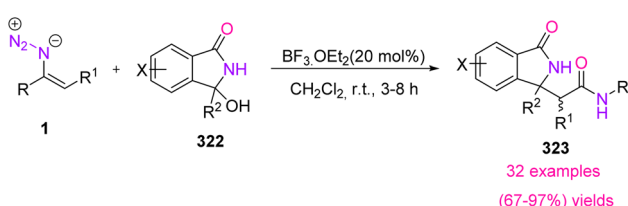
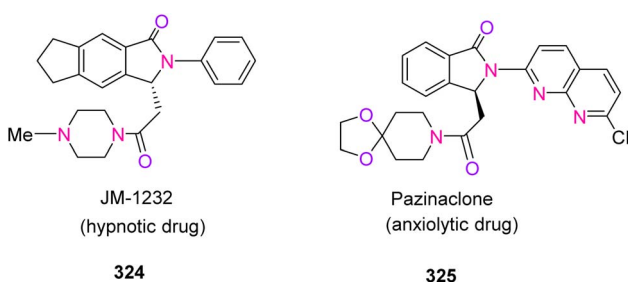
Scheme 90 Synthesis of 3-oxoisindoline-1-acetamides **323** via vinyl azides.

Fig. 8 Some biologically active isoindolinone derivatives.

bioactive compounds, drug leads, and chemical probes.<sup>103,104</sup> On the other hand, isoindolinones are the key structural unit present in numerous synthetically useful or naturally bioactive compounds, as shown in Fig. 8.<sup>105</sup>

In the mechanism of this reaction, *N*-acyl iminium salt intermediate **324** was first produced from 3-aryl-3-hydroxyisoindolineones, when  $\text{BF}_3 \cdot \text{Et}_2\text{O}$  was in the reaction vessel. The nucleophilic addition of vinyl azides to intermediate **324** generated iminodiazonium intermediate **325**. Then, intermediate **325** underwent Schmidt-type 1,2-migration, with the release of dinitrogen, to generate nitrilium ion intermediate **326**. Eventually, hydrolysis of this intermediate **326** gave product **323** (Scheme 91).<sup>102</sup>

In 2020, Szpilman *et al.* reported the indium(III)-catalyzed reaction of indole **327** and vinyl azides **1**, which led to the production of derivatives of **328** in fair to excellent yields (61–96%). In this strategy, another indole also reacted with **328** and produced **329** in fair to excellent yields (66–96%) (Scheme 92). This is the first displacement of the azide group by a carbon nucleophile while keeping the vinyl part. Extraordinarily, the substitution of azide on the  $\text{sp}^2$  carbon with the retention of the alkene system has not yet been disclosed. It would also be an attractive type of reactivity and would pioneer many new possibilities in chemistry.<sup>106</sup>

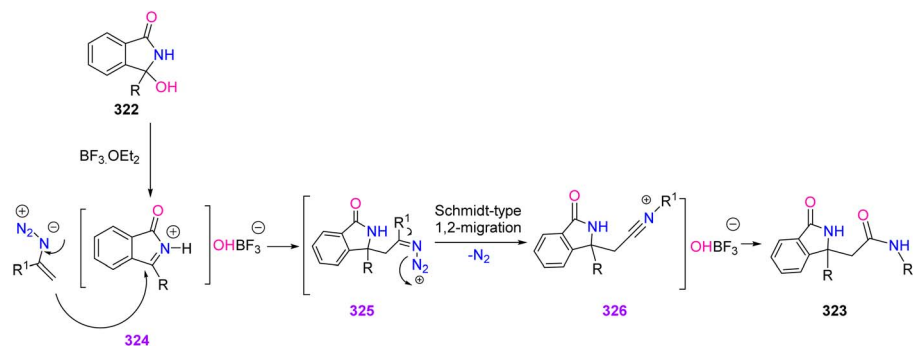
In such a process, it would be necessary to reversibly attach an electrophilic catalyst, *e.g.*, a Lewis acid, at the  $\alpha$ -position of vinyl azides **1**, generating an electrophilic diazoimine species **331**. The initial step would allow a nucleophile-like indole to attack the azide-bearing carbon in **331** with the generation of **333**.  $\text{E}_2$  elimination of indium trichloride and azide anion **335** would lead to the generation of charged species **334** and close the catalytic cycle. This step would likely be irreversible. In the final step, the azide anion would abstract a proton from **334** to generate the product vinyl indole **328** and hydrazoic acid (Scheme 93).<sup>106</sup>

In 2021, Dong Xu *et al.* reported an efficient synthesis of  $\beta$ -keto sulfides **337** through an aryl-thiol azide coupling reaction (Scheme 94). Diverse  $\beta$ -keto sulfides were produced through this method in poor to excellent yields (45–90%). Thiyl radicals have been well suited and broadly used in organic synthesis, but the reaction of vinyl azide with thiyl radical is rare.<sup>107</sup>

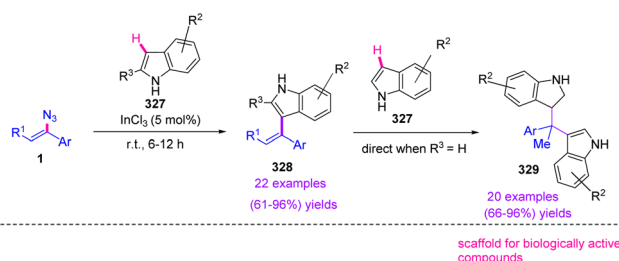
For the first time in 1997, Montecocchi and coworkers studied the reaction of thiols **336** and vinyl azides **1**. They found that the reaction of  $\alpha$ -phenyl vinyl azides with aryl thiols **336** was fast, producing  $\beta$ -keto sulfides **337** almost quantitatively. In this study, the authors proposed a radical-chain mechanism. First, aryl thiyl radical **338**, produced through the spontaneous oxidation of aryl thiol by oxygen, added to  $\beta$ -vinylic carbon of  $\alpha$ -phenyl vinyl azides with subsequent nitrogen extrusion to generate  $\beta$ -sulfanyliminyl radical **339**. Hydrogen abstraction from the next aryl thiol reproduced thiyl radical **338** and generated intermediate imine **340** and its tautomer **341** that were both hydrolyzed to desired product **337** (Scheme 95).<sup>107</sup>

In 2019, Fie Xu *et al.* developed an efficient method to obtain cyclic  $\beta$ -amino ketones **343** via visible-light photo-redox catalysis in poor to very good yields (18–82%).<sup>108</sup>  $\beta$ -Amino ketones are versatile synthetic building blocks in organic chemistry that can

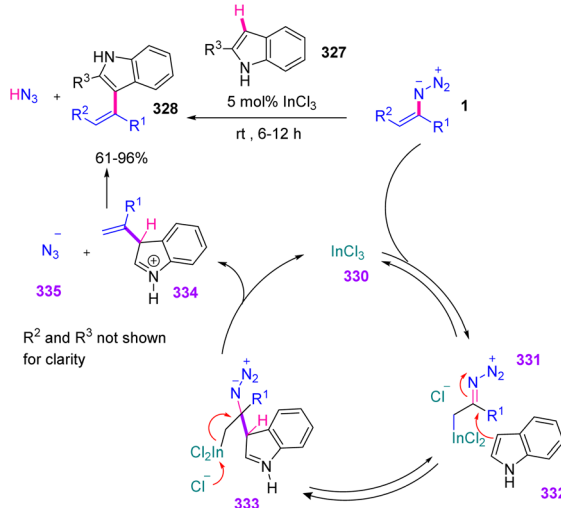




Scheme 91 Mechanism for the synthesis of 3-oxoisindoline-1-acetamides **323** through vinyl azides **1**.



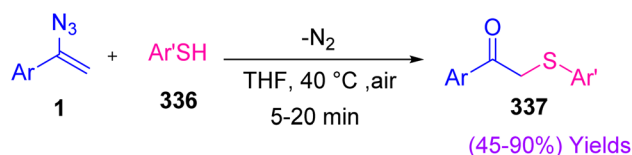
Scheme 92 Indium(III)-catalyzed reaction of indole **327** and vinyl azides **1**.



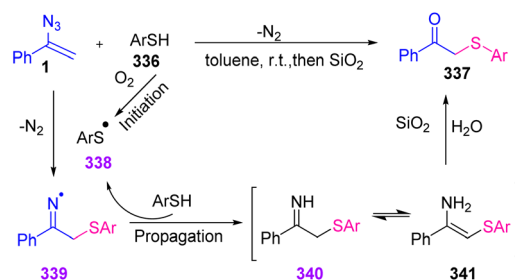
Scheme 93 Mechanism for the indium(III)-catalyzed reaction of indole **327** and vinyl azides **1**.

be converted into a range of beneficial and valuable derivatives containing  $\beta$ -amino-alcohols.  $\beta$ -Amino carbonyl derivatives are attractive as key synthetic intermediates of a wide range of drugs and biologically active natural products (Scheme 96).<sup>109</sup>

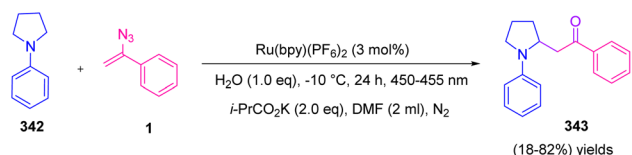
To illustrate the mechanism of this reaction, the single-electron transfer from the amine to visible-light-excited photocatalyst  $^*\text{Ru}(\text{bpy})_3^{2+}$  ( $^*\text{Ru}^{\text{II}}/\text{Ru}^{\text{I}} = 0.84 \text{ V}$ ) started the first catalytic cycle and prepared electron-rich  $\text{Ru}(\text{bpy})_3^+$  **346** and amine radical cation **347**. Then, the amine radical cation **347**



Scheme 94 Synthesis of  $\beta$ -keto sulfides through an aryl-thiol **336** azide coupling reaction.



Scheme 95 Mechanism for the synthesis of  $\beta$ -keto sulfides **337** through an aryl-thiol azide coupling reaction.

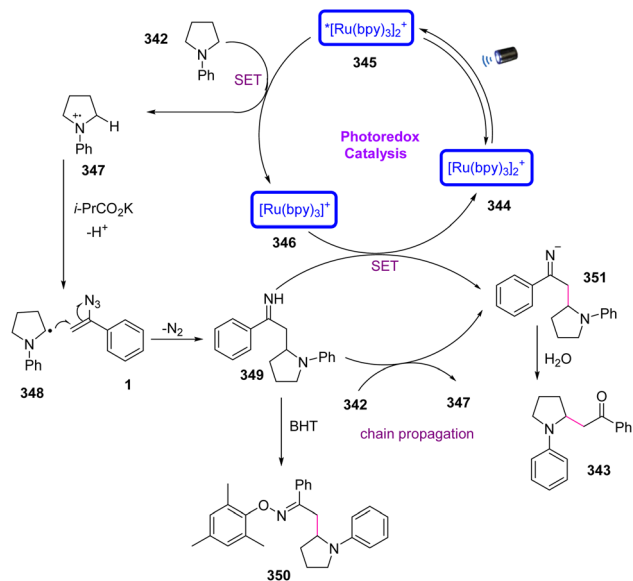


Scheme 96 Synthesis of  $\beta$ -amino ketones **343** via visible-light photo-redox catalysis.

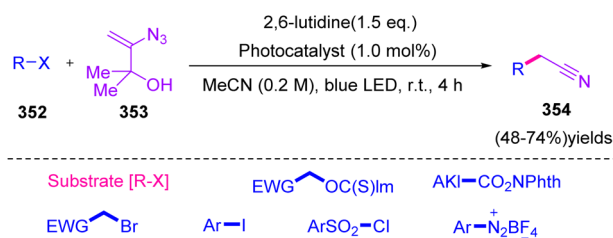
reacting with the base generated  $\alpha$ -amino radical **348**. The C-H bonds adjacent to the nitrogen atom in intermediate **347** underwent deprotonation by *i*-PrC O<sub>2</sub>K to generate  $\alpha$ -amino radical **348**. Radical addition of  $\alpha$ -amino radical **348** to vinyl azide gave iminyl radical **349**, which was reduced by the reductive photocatalyst to generate imine anion intermediate **351**. In the final step, hydrolysis of the imine anion **351** produced  $\beta$ -amino ketone **343** (Scheme 97).<sup>108</sup>

In 2019, Donald *et al.* proposed a novel strategy for radical cyanomethylation through vinyl azides **1** and produced diverse





Scheme 97 Mechanism for the synthesis of  $\beta$ -amino ketones **343** via visible-light photo-redox catalysis.

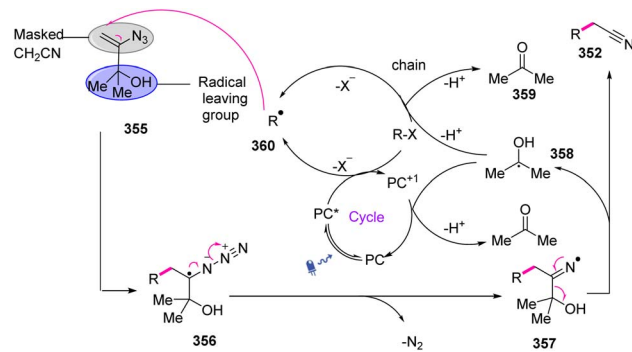


Scheme 98 Radical cyanomethylation through vinyl azide **353**.

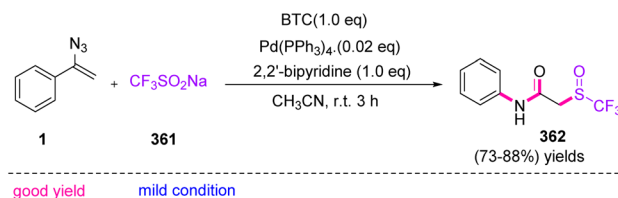
derivatives of **354** in fair to good yields (48–74%) (Scheme 98).<sup>110</sup> Nitrile groups are present in the structures of many pharmaceuticals and bioactive natural products.<sup>111</sup> Nitriles are also widely utilized as a directing group in C–H activation chemistry<sup>112</sup> and as versatile synthetic intermediates, especially as precursor to heterocycles<sup>113</sup> and functionalities at the carboxylic acid oxidation level.<sup>110</sup>

3-Azido-2-methylbut-3-en-2-ol **353** was considered an appropriate tool to achieve the cyanomethylation of radicals due to it encompassing two key design elements: (I) vinyl azides **1** that can act as masked cyanomethyl groups, and (II) dimethyl carbinol as a latent radical leaving group. With radical generation from a substrate through the oxidative quenching of an excited-state photo-redox catalyst ( $PC^* \rightarrow PC^{1+}$ ), it was anticipated that reagent **355** would intercept open-shell species to initiate a cascade process *via* radical addition to the olefin, producing adduct **356** that would release dinitrogen to produce iminyl radical **357**. In the next step, fragmentation of iminyl radical **357** *via*  $\alpha$ -C–C bond cleavage and ejection of the 2-hydroxypropyl radical **358** was expected to produce nitrile functionality (Scheme 99).<sup>110</sup>

In 2022, Tang *et al.* synthesized *N*-aryl-(trifluoromethyl sulfinyl) acetamides **362** in good to very good yields (73–88%),



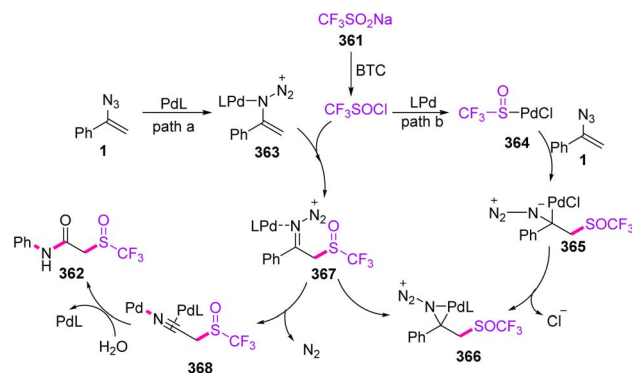
Scheme 99 Mechanism for radical cyanomethylation through vinyl azides **353**.



Scheme 100 Synthesis of *N*-aryl-(trifluoromethyl sulfinyl) acetamides **362** from vinyl azides.

through *S*-triggered Schmidt-type rearrangement of vinyl azides **1** (Scheme 100).<sup>114</sup> The trifluoromethylthio ( $CF_3S$ ) functional group is very common in the structures of agrochemical<sup>115</sup> compounds, such as fipronil, toltrazuril, triflorex, and cefazafur, and medicinal compounds, improving physio-chemical properties and pharmacokinetics, owing to their electron-negativity and excellent lipophilicity.<sup>116</sup>

As depicted in Scheme 101, a Pd(0) catalyst first activated vinyl azides **1** to give metal complex **363** *via* path a. Addition of  $CF_3SOCl$ , *in situ* generated from the reaction of  $CF_3SO_2Na$  with BTC, to the palladium-activated intermediate **363** happened to form the C–S bond, giving imine species **367**. On the other hand, path b suggested that the PdL complex might be inserted into the  $CF_3SO-Cl$  bond through oxidative addition to give intermediate **364**. Then, substrate **1** coordinated to metal



Scheme 101 Mechanism for the synthesis of *N*-aryl-(trifluoromethyl sulfinyl) acetamides **362**.

Table 3 Synthesis of other compounds through vinyl azides

| Catalyst (mol%)  | Solvent                         | Temperature | MW irradiation | Yield  | Reference                  |
|--|---------------------------------|-------------|----------------|--------|----------------------------|
| Ir[(COD)Cl] <sub>2</sub> (3 mol%)                              | THF                             | 50 °C       | ✗              | 40–75% | Mukherjee <sup>79</sup>    |
| Eosin Y (1–10 mol%)  | EtOH                            | r.t.        | ✓              | 38–68% | O. Terent'ev <sup>80</sup> |
| Taking advantage of non-catalytic amount of CAN                | MeOH                            | r.t.        | ✗              | 54–88% | O. Terent'ev <sup>81</sup> |
| No cat.  | DCE                             | 110 °C      | ✗              | 58–88% | Fan <sup>85</sup>          |
| Mn(acac) <sub>3</sub> (20 mol%)                                | NMP                             | 60 °C       | ✗              | 65–92% | Yu <sup>87</sup>           |
| Cu(OAc) <sub>2</sub> (15 mol%)                                 | DMSO                            | 40 °C       | ✗              | 72–96% | Tang <sup>91</sup>         |
| CuCl <sub>2</sub> ·H <sub>2</sub> O (10 mol%)                  | DMSO                            | 80 °C       | ✗              | 59–89% | Wang <sup>95</sup>         |
| I <sub>2</sub> (50 mol%)                                       | CH <sub>3</sub> CN              | r.t.        | ✗              | 57–86% | Dandela <sup>5</sup>       |
| Taking advantage of non-catalytic amount of Ag NO <sub>2</sub> | 1,4-Dioxane                     | 60 °C       | ✗              | 63–91% | Bi <sup>101</sup>          |
| Ag NO <sub>3</sub> (20 mol%)                                   | NMP                             | 60 °C       | ✗              | 37–62% |                            |
| CuI (10 mol%)  | CH <sub>3</sub> CN              | 70 °C       | ✗              | 60–87% |                            |
| BF <sub>3</sub> ·OEt <sub>2</sub> (20 mol%)                    | CH <sub>2</sub> Cl <sub>2</sub> | r.t.        | ✗              | 67–97% | Singh <sup>102</sup>       |
| InCl <sub>3</sub> (5 mol%)                                     | DCM                             | r.t.        | ✗              | 61–96% | Szpilman <sup>106</sup>    |
| No cat.  | THF                             | 40 °C       | ✗              | 45–90% | Dong <sup>107</sup>        |
| Ru(bpy)(PF <sub>6</sub> ) <sub>2</sub> (3 mol%)                | DMF                             | –10 °C      | ✓              | 18–82% | Fie <sup>108</sup>         |
| Photocatalyst (1 mol%)   | CH <sub>3</sub> CN              | r.t.        | ✓              | 48–74% | Donald <sup>110</sup>      |
| Pd(PPh <sub>3</sub> ) <sub>4</sub> (2 mol%)                    | CH <sub>3</sub> CN              | r.t.        | ✗              | 73–88% | Tang <sup>114</sup>        |

complex **364** for the synthesis of **365**, proceeding to intra-molecular migratory insertion to generate species **366**. This complex **366** could be isomerized into intermediate **367**. Then, intermediate **367** underwent Schmidt-type 1,2-phenyl migration together with extrusion of N<sub>2</sub> to give nitrilium ion **368**. In the final step, trace H<sub>2</sub>O in the solvent intercepted the reactive intermediate **368** to complete the process *via* hydration that gave the desired product **362**.<sup>114</sup>

Table 3 was prepared to provide a summary of the strategies researchers have utilized to synthesize other compounds through vinyl azides, in which catalyst, solvent, temperature, yield, and MW irradiation are compared.

## Conclusion

Vinyl azides as versatile synthons are applied for the synthesis of different types of compounds, such as cyclic, heterocyclic, and non-cyclic compounds. *N*-heterocycles are a group of nitrogen-containing compounds with a broad range of interesting biological and pharmaceutical applications. Due to their high and diverse reactivity, vinyl azides are promising candidates as precursors for the production of *N*-heterocycles. It is our belief that utilizing this three-atom synthon in new protocols for the synthesis of heterocyclic compounds and other pharmaceutical compounds will continue to progress in coming years.

## Conflicts of interest

There are no conflicts to declare.

## Notes and references

- G. Smolinsky and C. Pryde, *J. Org. Chem.*, 1968, **33**, 2411–2416.
- J. Cen, J. Li, Y. Zhang, Z. Zhu, S. Yang and H. Jiang, *Org. Lett.*, 2018, **20**, 4434–4438.
- K. V. Sajna and K. K. Swamy, *J. Org. Chem.*, 2012, **77**, 8712–8722.
- Z. Li, T. Huo, L. Li, S. Feng, Q. Wang, Z. Zhang, S. Pang, Z. Zhang, P. Wang and Z. Zhang, *Org. Lett.*, 2018, **20**, 7762–7766.
- S. Bhukta, R. Chatterjee and R. Dandela, *Org. Biomol. Chem.*, 2022, **20**, 3907–3912.
- D. J. Duarte, M. S. Miranda and J. C. Esteves da Silva, *J. Phys. Chem. A*, 2014, **118**, 5038–5045.
- G. L'Abbe and G. Mathys, *J. Org. Chem.*, 1974, **39**, 1778–1780.
- R. G. Ford, *J. Mol. Spectrosc.*, 1977, **65**, 273–279.
- C. Lin, Y. Shen, B. Huang, Y. Liu and S. Cui, *J. Org. Chem.*, 2017, **82**, 3950–3956.
- N. Thirupathi, C. H. Tung and Z. Xu, *Adv. Synth. Catal.*, 2018, **360**, 3585–3589.
- G. L'abbe, *Chem. Rev.*, 1968, **69**, 345–363.
- G. Favini and R. Todeschini, *J. Mol. Struct.*, 1978, **50**, 191–193.
- R. R. Donthiri, *Org. Biomol. Chem.*, 2015, **13**, 10113–10116.
- R. B. Thompson, *FASEB J.*, 2001, **15**, 1671–1676.
- A. Fürstner, *Angew. Chem., Int. Ed.*, 2003, **42**, 3582–3603.
- H. Nishida, A. Hasuoka, Y. Arikawa, O. Kurasawa, K. Hirase, N. Inatomi, Y. Hori, F. Sato, N. Tarui, A. Imanishi and M. Kondo, *Bioorg. Med. Chem.*, 2012, **20**, 3925–3938.
- J. Cen, Y. Wu, J. Li, L. Huang, W. Wu, Z. Zhu, S. Yang and H. Jiang, *Org. Lett.*, 2019, **21**, 2090–2094.
- R. Chinchilla and C. Nájera, *Chem. Rev.*, 2007, **107**, 874–922.
- K. Huang, C. L. Sun and Z. J. Shi, *Chem. Soc. Rev.*, 2011, **40**, 2435–2452.
- W. L. Lei, K. W. Feng, T. Wang, L. Z. Wu and Q. Liu, *Org. Lett.*, 2018, **20**, 7220–7224.
- R. H. Feling, G. O. Buchanan, T. J. Mincer, C. A. Kauffman, P. R. Jensen and W. Fenical, *Angew. Chem., Int. Ed.*, 2003, **42**, 355–357.





- 22 G. I. Ioannou, T. Montagnon, D. Kalaitzakis, S. A. Pergantis and G. Vassilikogiannakis, *ChemPhotoChem*, 2018, **2**, 860–864.
- 23 D. Kalaitzakis, M. Sofiadis, M. Triantafyllakis, K. Daskalakis and G. Vassilikogiannakis, *Org. Lett.*, 2018, **20**, 1146–1149.
- 24 Y. Q. Tang, J. C. Yang, L. Wang, M. Fan and L. N. Guo, *Org. Lett.*, 2019, **21**, 5178–5182.
- 25 Y. Wang, Z. Li, H. Zhao and Z. Zhang, *Synth.*, 2019, **51**, 3250–3258.
- 26 P. I. Hernández, D. Moreno, A. A. Javier, T. Torroba, R. Pérez-Tomás and R. Quesada, *Chem. Commun.*, 2012, **48**, 1556–1558.
- 27 S. A. Parikh, H. Kantarjian, A. Schimmer, W. Walsh, E. Asatiani, K. El-Shami, E. Winton and S. Verstovsek, *Clin. Lymphoma, Myeloma Leuk.*, 2010, **10**, 285–289.
- 28 R. R. Donthiri, V. Pappula, N. N. K. Reddy, D. Bairagi and S. Adimurthy, *J. Org. Chem.*, 2014, **79**, 11277–11284.
- 29 C. Enguehard-Gueiffier and A. Gueiffier, *Mini-Rev. Med. Chem.*, 2007, **7**, 888–899.
- 30 K. C. Rupert, J. R. Henry, J. H. Dodd, S. A. Wadsworth, D. E. Cavender, G. C. Olini, B. Fahmy and J. J. Siekierka, *Bioorg. Med. Chem. Lett.*, 2003, **13**, 347–350.
- 31 F. Chen, T. Shen, Y. Cui and N. Jiao, *Org. Lett.*, 2012, **14**, 4926–4929.
- 32 C. T. Walsh, S. Garneau-Tsodikova and A. R. Howard-Jones, *Nat. Prod. Rep.*, 2006, **23**, 517–531.
- 33 P. Novák, K. Müller, K. S. V. Santhanam and O. Haas, *Chem. Rev.*, 1997, **97**, 207–281.
- 34 J. E. Curiel Tejeda, L. C. Irwin and M. A. Kerr, *Org. Lett.*, 2016, **18**, 4738–4741.
- 35 L. Jie, L. Wang, D. Xiong, Z. Yang, D. Zhao and X. Cui, *J. Org. Chem.*, 2018, **83**, 10974–10984.
- 36 L. Li, Z. Chen, X. Zhang and Y. Jia, *Chem. Rev.*, 2018, **118**, 3752–3832.
- 37 S. Chiba, Y. F. Wang, G. Lapointe and K. Narasaka, *Org. Lett.*, 2008, **10**, 313–316.
- 38 Z. Zhu, X. Tang, J. Li, X. Li, W. Wu, G. Deng and H. Jiang, *Org. Lett.*, 2017, **19**, 1370–1373.
- 39 K. J. Shaw, P. W. Erhardt, A. A. Hagedorn III, C. A. Pease, W. R. Ingebretsen and J. R. Wiggins, *J. Med. Chem.*, 1992, **35**, 1267–1272.
- 40 M. Kozaki, A. Isoyama and K. Okada, *Tetrahedron Lett.*, 2006, **47**, 5375–5378.
- 41 E. J. Corey, D. H. Lee and S. Sarshar, *Tetrahedron: Asymmetry*, 1995, **6**, 3–6.
- 42 D. B. Ramachary, G. S. Reddy, S. Peraka and J. Gujral, *ChemCatChem*, 2017, **9**, 263–267.
- 43 T. Tsuritani, H. Mizuno, N. Nonoyama, S. Kii, A. Akao, K. Sato, N. Yasuda and T. Mase, *Org. Process Res. Dev.*, 2009, **13**, 1407–1412.
- 44 B. Gopalan and K. K. Balasubramanian, *Click React. Org. Synth.*, 2016, 25–76.
- 45 Z. Liu, H. Ji, W. Gao, G. Zhu, L. Tong, F. Lei and B. Tang, *Chem. Commun.*, 2017, **53**, 6259–6262.
- 46 R. Cai, W. Yan, M. G. Bologna, K. de Silva, Z. Ma, H. O. Finklea, J. L. Petersen, M. Li and X. Shi, *Org. Chem. Front.*, 2015, **2**, 141–144.
- 47 Q. Gu, H. H. Al Mamari, K. Graczyk, E. Diers and L. Ackermann, *Angew. Chem., Int. Ed.*, 2014, **53**, 3868–3871.
- 48 W. Wu, Q. Chen, Y. Tian, Y. Xu, Y. Huang, Y. You and Z. Weng, *Org. Chem. Front.*, 2020, **7**, 1878–1883.
- 49 A. Sysak and B. Obmińska-Mrukowicz, *Eur. J. Med. Chem.*, 2017, **137**, 292–309.
- 50 C. Lamberth, *J. Heterocycl. Chem.*, 2018, **55**, 2035–2045.
- 51 J. Lin, W. Wu and Z. Weng, *Tetrahedron Lett.*, 2020, **61**, 152672.
- 52 F. Giornal, S. Pazenok, L. Rodefeld, N. Lui, J. P. Vors and F. R. Leroux, *J. Fluorine Chem.*, 2013, **152**, 2–11.
- 53 N. A. Meanwell, *J. Med. Chem.*, 2011, **54**, 2529–2591.
- 54 Z. Zhang, R. K. Kumar, G. Li, D. Wu and X. Bi, *Org. Lett.*, 2015, **17**, 6190–6193.
- 55 P. Zhou, Y. Huang, W. Wu, W. Yu, J. Li, Z. Zhu and H. Jiang, *Org. Biomol. Chem.*, 2019, **17**, 3424–3432.
- 56 K. Okonogi, M. Kuno, M. Kida and S. Mitsunashi, *Antimicrob. Agents Chemother.*, 1981, **20**, 171–175.
- 57 M. L. Zhu, C. M. Horbinski, M. Garzotto, D. Z. Qian, T. M. Beer and N. Kyprianou, *Cancer Res.*, 2010, **70**, 7992–8002.
- 58 B. Chen, S. Guo, X. Guo, G. Zhang and Y. Yu, *Org. Lett.*, 2015, **17**, 4698–4701.
- 59 S. Annadurai, R. Martinez, D. J. Canney, T. Eidem, P. M. Dunman and M. Abou-Gharbia, *Bioorg. Med. Chem. Lett.*, 2012, **22**, 7719–7725.
- 60 B. Smith, H. H. Chang, F. Medda, V. Gokhale, J. Dietrich, A. Davis, E. J. Meuillet and C. Hulme, *Bioorg. Med. Chem. Lett.*, 2012, **22**, 3567–3570.
- 61 S. Arutyunyan and A. Nefzi, *J. Comb. Chem.*, 2010, **12**, 315–317.
- 62 J. C. Yang, J. Y. Zhang, J. J. Zhang, X. H. Duan and L. N. Guo, *J. Org. Chem.*, 2018, **83**, 1598–1605.
- 63 B. Zhang and A. Studer, *Chem. Soc. Rev.*, 2015, **44**, 3505–3521.
- 64 J. Wang, D. Ba, M. Yang, G. Cheng and L. Wang, *J. Org. Chem.*, 2021, **86**, 6423–6432.
- 65 E. Kiselev, K. Agama, Y. Pommier and M. Cushman, *J. Med. Chem.*, 2012, **55**, 1682–1697.
- 66 P. Schlagenhauf, M. Adamcova, L. Regep, M. T. Schaerer and H. G. Rhein, *Malar. J.*, 2010, **9**, 1–15.
- 67 Z. Zhu, X. Tang, X. Li, W. Wu, G. Deng and H. Jiang, *J. Org. Chem.*, 2016, **81**, 1401–1409.
- 68 L. L. Mao, D. G. Zheng, X. H. Zhu, A. X. Zhou and S. D. Yang, *Org. Chem. Front.*, 2018, **5**, 232–236.
- 69 K. Liu, S. Chen, X. G. Li and P. N. Liu, *J. Org. Chem.*, 2016, **81**, 265–270.
- 70 K. Muller, C. Faeh and F. Diederich, *Science*, 2007, **317**, 1881–1886.
- 71 B. Nie, W. Wu, C. Jin, Q. Ren, J. Zhang, Y. Zhang and H. Jiang, *J. Org. Chem.*, 2022, **87**, 159–171.
- 72 M. Yang, X. H. Meng, Z. Wang, Y. Gong and Y. L. Zhao, *Org. Chem. Front.*, 2020, **7**, 3493–3498.
- 73 J. C. Yang, J. J. Zhang and L. N. Guo, *Org. Biomol. Chem.*, 2016, **14**, 9806–9813.
- 74 C. S. Yeung and V. M. Dong, *Chem. Rev.*, 2011, **111**, 1215–1292.





- 75 U. K. Das, L. J. Shimon and D. Milstein, *Chem. Commun.*, 2017, **53**, 13133–13136.
- 76 Y. F. Wang and S. Chiba, *J. Am. Chem. Soc.*, 2009, **131**, 12570–12572.
- 77 H. X. Siyang, X. Y. Ji, X. R. Wu, X. Y. Wu and P. N. Liu, *Org. Lett.*, 2015, **17**, 5220–5223.
- 78 G. Chianese, E. Fattorusso, O. Taglialatela-Scafati, G. Bavestrello, B. Calcinai, H. A. Dien, A. Ligresti and V. Di Marzo, *Steroids*, 2011, **76**, 998–1002.
- 79 A. Chakrabarty and S. Mukherjee, *Org. Lett.*, 2020, **22**, 7752–7756.
- 80 O. M. Mulina, A. I. Ilovaisky, T. Opatz and A. O. Terent'ev, *Tetrahedron Lett.*, 2021, **64**, 152737.
- 81 S. A. Paveliev, L. S. Alimkhanova, A. V. Sergeeva and A. O. Terent'ev, *Tetrahedron Lett.*, 2020, **61**, 152533.
- 82 E. G. Bagryanskaya and S. R. Marque, *Chem. Rev.*, 2014, **114**, 5011–5056.
- 83 L. Tebben and A. Studer, *Angew. Chem., Int. Ed.*, 2011, **50**, 5034–5068.
- 84 R. Ciriminna and M. Pagliaro, *Org. Process Res. Dev.*, 2010, **14**, 245–251.
- 85 C. Gao, Q. Zhou, L. Yang, X. Zhang and X. Fan, *J. Org. Chem.*, 2020, **85**, 13710–13720.
- 86 A. Białas, J. Grembecka, D. Krowarsch, J. Otlewski, J. Potempa and A. Mucha, *J. Med. Chem.*, 2006, **49**, 1744–1753.
- 87 P. Tang, C. Zhang, E. Chen, B. Chen, W. Chen and Y. Yu, *Tetrahedron Lett.*, 2017, **58**, 2157–2161.
- 88 C. Queffelec, M. Petit, P. Janvier, D. A. Knight and B. Bujoli, *Chem. Rev.*, 2012, **112**, 3777–3807.
- 89 P. Zhang, L. Zhang, Y. Gao, J. Xu, H. Fang, G. Tang and Y. Zhao, *Chem. Commun.*, 2015, **51**, 7839–7842.
- 90 W. Wei and J. X. Ji, *Angew. Chem.*, 2011, **123**, 9263–9265.
- 91 Z. Liu, Z. Zhang, G. Zhu, Y. Zhou, L. Yang, W. Gao, L. Tong and B. Tang, *Org. Lett.*, 2019, **21**, 7324–7328.
- 92 M. Müller, C. M. Orben, N. Schützenmeister, M. Schmidt, A. Leonov, U. M. Reinscheid, B. Dittrich and C. Griesinger, *Angew. Chem., Int. Ed.*, 2013, **52**, 6047–6049.
- 93 J. W. Corbett, S. S. Ko, J. D. Rodgers, L. A. Gearhart, N. A. Magnus, L. T. Bacheler, S. Diamond, S. Jeffrey, R. M. Klabe, B. C. Cordova and S. Garber, *J. Med. Chem.*, 2000, **43**, 2019–2030.
- 94 G. M. Keating and A. Santoro, *Drugs*, 2009, **69**, 223–240.
- 95 Y. Zhang, M. Luo, Y. Zhang, K. Cheng, Y. Li, C. Qi, R. Shen and H. Wang, *Org. Biomol. Chem.*, 2022, **20**, 1952–1957.
- 96 L. Deng, X. Cao, Y. Liu and J. P. Wan, *J. Org. Chem.*, 2019, **84**, 14179–14186.
- 97 P. A. Vigato, V. Peruzzo and S. Tamburini, *Coord. Chem. Rev.*, 2009, **253**, 1099–1201.
- 98 A. G. Montalban, E. Boman, C. D. Chang, S. C. Ceide, R. Dahl, D. Dalesandro, N. G. Delaet, E. Erb, J. T. Ernst, A. Gibbs and J. Kahl, *Bioorg. Med. Chem. Lett.*, 2010, **20**, 4819–4824.
- 99 C. Steuer, C. Gege, W. Fischl, K. H. Heinonen, R. Bartenschlager and C. D. Klein, *Bioorg. Med. Chem.*, 2011, **19**, 4067–4074.
- 100 Y. Kim, A. C. G. Kankanamalage, V. C. Damalanka, P. M. Weerawarna, W. C. Groutas and K. O. Chang, *Antiviral Res.*, 2016, **125**, 84–91.
- 101 Y. Ning, X. F. Zhao, Y. B. Wu and X. Bi, *Org. Lett.*, 2017, **19**, 6240–6243.
- 102 D. Kumar Das, V. K. Kannaujiya, M. M. Sadhu, S. K. Ray and V. K. Singh, *J. Org. Chem.*, 2019, **84**, 15865–15876.
- 103 C. J. Gerry and S. L. Schreiber, *Nat. Rev. Drug Discovery*, 2018, **17**, 333–352.
- 104 L. Arzel, D. Dubreuil, F. Dénès, V. Silvestre, M. Mathe-Allainmat and J. Lebreton, *J. Org. Chem.*, 2016, **81**, 10742–10758.
- 105 K. Speck and T. Magauer, *Beilstein J. Org. Chem.*, 2013, **9**, 2048–2078.
- 106 A. A. More and A. M. Szpilman, *Org. Lett.*, 2020, **22**, 3759–3764.
- 107 Y. Wang, Y. J. Wang, X. C. Liang, M. H. Shen, H. D. Xu and D. Xu, *Org. Biomol. Chem.*, 2021, **19**, 5169–5176.
- 108 J. T. Xu, G. Q. Xu, Z. Y. Wang and P. F. Xu, *J. Org. Chem.*, 2019, **84**, 14760–14769.
- 109 E. Buchdunger, U. Trinks, H. Mett, U. Regenass, M. Müller, T. Meyer, E. McGlynn, L. A. Pinna, P. Traxler and N. B. Lydon, *Proc. Natl. Acad. Sci. U. S. A.*, 1994, **91**, 2334–2338.
- 110 J. R. Donald and S. L. Berrell, *Chem. Sci.*, 2019, **10**, 5832–5836.
- 111 F. F. Fleming, L. Yao, P. C. Ravikumar, L. Funk and B. C. Shook, *J. Med. Chem.*, 2010, **53**, 7902–7917.
- 112 B. Heller and M. Hapke, *Chem. Soc. Rev.*, 2007, **36**, 1085–1094.
- 113 P. J. Lindsay-Scott and P. T. Gallagher, *Tetrahedron Lett.*, 2017, **58**, 2629–2635.
- 114 Z. Liu, T. Yu, L. Li, W. Fu, X. Gan, H. Chen, W. Gao and B. Tang, *Org. Chem. Front.*, 2022, **9**, 1241–1246.
- 115 D. O'Hagan, *Chem. Soc. Rev.*, 2008, **37**, 308–319.
- 116 F. Leroux, P. Jeschke and M. Schlosser, *Chem. Rev.*, 2005, **105**, 827–856.

